L-band RFI Measurement System Simulation and Investigation

Andile Mngadi

A dissertation submitted to the Department of Electrical Engineering,
University of Cape Town, in fulfilment of the requirements
for the degree of Master of Science in Engineering.

Cape Town, February 2007

Declaration

I declare that this thesis is my own, unaided work. It is submitted in fulfilment of the requirements for the degree of Master of Science in Engineering at the University of Cape Town. It has not been submitted before for any degree or examination in any other university.

Signature of Author .. Signed by candidate .....

Department of Electrical Engineering,

Cape Town, February 2007

Abstract

The Square Kilometre Array (SKA) is a multi billion dollar international project to create *a receiving surface of a million square metres, one hundred times larger than the biggest receiving surface now in existence.* The SKA core array will have to be located in a **remote area**. Therefore countries interested in hosting the SKA core array were requested to perform Radio Frequency Interference measurements at their site of choice. The systems that are to be used in the measurements must conform to a document called the "RFI Measurement Protocol for Candidates SKA Sites", the SKA Memo 37.

The RFI protocol divides measurements into two parts, Mode 1 and Mode 2. *Mode 1* is defined for the observation of strong RFI and is relevant for SKA receiver linearity analysis. *Mode 2* is defined for the observation of weak interferences, which potentially threatens to obscure weak signals of interest.

In Mode 1, the RFI protocol specifies a dwell time of 2 μs duration over a large 1 MHz bandwidth in the 960 -1400 MHz band (L-band). The reason for this short dwell time is to capture and characterize pulsed interference from radars and Distance Measuring Equipment (DME) in this band. This kind of interference is expected, potentially with very high peak power and short dwell time. Executing these measurements with the spectrum analyzer is impractical because of the very long measurement times. It was therefore proposed to build a dedicated FFT spectrometer from standard components, state of the art FPGA board with a high speed 14 bit ADC.

The proposed system was designed by Dr. Adrian Tiplady and is called the RFI measurement system 4. This thesis investigates whether system 4 measures impulsive RFI as required by the protocol. This was done by simulating the receiver of system 4 and feeding the receiver with simulated DME signals. The simulated receiver findings were then compared to the real receiver findings when similar DME-like signals were injected into the real receiver.

The practical system was found to be able to withstand high power signals from DME systems without suffering from compression and inter-modulation distortion. The maximum signal that the receiver can handle under automatic gain control is 9 dBm, equivalent to 8 mW into 50 Ohms. However, the automatic gain mode was found not to be desirable for RFI measurements because of the unknown gain in the AGC. The simulated receiver was found to measure RFI as expected by the protocol without any compression and inter-modulation distortion. Manual mode is recommended for making level measurements in

absolute terms.

Acknowledgements

A big thank you to my supervisor, Professor Michael R. Inggs, for giving me a chance to be involved in this project. I am very thankful for his wisdom and guidance throughout the project period. I am also very grateful to Dr. Richard T. Lord for his contributions in this thesis.

Without the financial assistance from the South African SKA project office, I would not have been able to undertake and complete this project, for that I am grateful. I am very thankful to the S.A. SKA RFI team for the support they provided.

Thank you to my colleagues in the RRSG for making the environment conducive for research, even at the worst of times. I am indebted to my friends for keeping me sane, living under the harsh conditions of academics, scientists and engineers.

To my family, for sharing my vision, your support is very much appreciated.

Contents

List of Figures

List of Tables

List of Symbols

Symbol	Definition
μ	Micro
t	Time
λ	Wavelength
f	Frequency
f_{3dB}	3 dB cut-off frequency
f_s	Sampling frequency
f_{max}	Maximum frequency
f_{ADC}	Analogue to Digital Converter's sampling frequency
f_{DME}	Frequency of the Distance Measuring Equipment
C_{OFS}	Capacitance at the offset nulling points of the compensation loop
DR_r	Dynamic Range of a receiver
G	Gain
G_{acc}	Accumulated Gain in a receiver chain
G_r	Gain of the receiving antenna
G_{sys}	Gain of the receiving system
G_t	Gain of the transmitter's antenna
G_{AD8347}	Gain of the AD8347 demodulator
$G_{AD8347\text{-}max}$	Maximum Gain of the AD8347 demodulator
$G_{AD8347\text{-}min}$	Minimum Gain of the AD8347 demodulator
G_{IF}	Gain of the IF amplifier

G_{IFVGA}	Gain of the variable gain IF amplifier
G_{RFVGA}	Gain of the variable gain RF amplifier
G_{LNA}	Gain of the low noise amplifier
$G_{\text{VGA-max}}$	Maximum Gain of the Variable Gain Amplifier
$G_{\text{VGA-min}}$	Minimum Gain of the Variable Gain Amplifier
G_{WBAMP}	Gain of the wide-band amplifier
L	loss of a component
L_{acc}	Accumulated loss in a receiver chain
L_c	Conversion loss of a mixer
L_{cables}	Loss due to cables
L_{filter}	Loss due to a filter
L_{switches}	Loss due to switches
$L_{\text{switchcables}}$	Loss due to switch cables
N_{rep}	Number of repetitions of a measurement cycle
P	Power
P_1	1 dB gain compression point of either a mixer or an amplifier.
P_3	Third-order intercept point of either a mixer or amplifier.
P_{avg}	Average power
$P_{\text{mixer-out}}$	Power at the mixer output
$P_{\text{r-smallest}}$	Smallest receivable signal power
P_t	Transmitter Power
P_r	Received Power
P_{out}	Power out
P_{RFin}	Input Power of a signal at RF frequency
R	Range or distance
S_{0h}	Flux density over the horizon
T_{ADC}	Sampling period of the Analogue to Digital Converter

T_R	Receiver temperature
$V(t)$	Voltage as a function of time
W	Full-width half-amplitude of a Gaussian-shaped pulse

Nomenclature

ADC Analogue to Digital converter

AGC Automatic Gain Control

CW Continuous Waveform

DME Distance Measuring Equipment

DSB Double Side-Band

DST Department of Science and Technology

FFT Fast Fourier Transform

FPGA Field Programmable Gate Array

HartRAO Hartebeesthoek Radio Astronomy Observatory

IC Integrated Circuit

ICASA Independent Communications Authority of South Africa

IF Intermediate Frequency

IIR Infinite Impulse Response

ISPO International SKA Project Office

ITU International Telecommunications Union

L-band Frequency band between 1 - 2 GHz

LNA Low Noise Amplifier

LO Local Oscillator

MHz Mega Hertz

MSPS Mega samples per seconds

NF Noise Figure

NRF National Research Foundation

RA Radio Astronomy

RF Radio Frequency

RFI Radio Frequency Interference

RSA Republic of South Africa

SA South Africa

SKA Square Kilometer Array

SSESC SKA Site Evaluation and Selection Committee

TV Television

VGA Variable Gain Amplifier

Chapter 1

Introduction

SKA stands for Square Kilometre Array. The SKA is a multi billion dollar international project to create *a receiving surface of a million square metres, one hundred times larger than the biggest receiving surface now in existence* [1]. The Republic of South Africa (RSA) has been short-listed as one of the two countries that might host the SKA core array. The SKA core array will have to be located in a **remote area**. This is because, relevant radio emissions from the early universe are in the range of a few hundred Mega Hertz, a frequency band now crowded on earth with TV and cellular telephone transmissions [1]. Because of this extremely high sensitivity required by this instrument, we cannot rely on the general spectrum protection criteria that the International Telecommunications Union (ITU) Radio Regulations specify in RA 769 for the several very specific parts of the radio frequency spectrum. Therefore countries contending for the core array must perform Radio Frequency Interference (RFI) measurements. The RFI measurements must conform to a document called the **SKA Memo 37, "RFI Measurement Protocol for Candidate SKA Sites"** [2], herein referred to as "the RFI protocol". The RFI protocol was established for the measurement and reporting of RFI at a single site for the use in the SKA site evaluation process by the SKA Site Evaluation and Selection Committee (SSESC).

The RF circuitry of the SA RFI measurement systems was designed by Dr. George Nicolson based on the requirements of the protocol, and was assembled and constructed by the Hartebeesthoek Radio Astronomy Observatory (HartRAO) staff [3]. When this thesis project was proposed the RFI measurement sets were experiencing a number of design problems. Among other problems, the 960-1400 MHz band (L-band) measurements took longer because of the spectrum analyzer readout time to the dwell time. An option to build a dedicated FFT spectrometer was then proposed. The proposed system was to be called the RFI Measurement system 4. This thesis project therefore investigates whether the L-band receiver of the RFI measurement system 4 meets the requirements of the protocol and measures the desired man-made "external" RFI as required by the RFI protocol. Therefore the thesis objectives are as follows.

1.1 Thesis Objectives

The objectives of this thesis project are as follows:

1. Review, understand and briefly describe the SKA RFI measurement protocol, both the average and the burst mode systems.
2. Review the receiver design of the three SA RFI measurement systems that were used for RFI measurements, by the SA RFI team, in the bidding process for the SKA core array.
3. Review the specifications of the proposed RFI measurement system 4 for the 960-1400 MHz frequency band which uses the Fast Fourier Transform (FFT) spectrometer. It is essential to note that the measurement of RFI using the FFT spectrometer is not specified by the protocol.
4. Produce a simulation of the proposed L-band RFI measurement system 4 receiver using Elanix's SystemView package.
5. Comment on the performance of the simulated receiver by checking if the RF circuitry of the proposed receiving system meets the requirements of the SKA protocol.
6. Predict by way of research the likely burst mode interferences in the L-band.
7. Check using the simulation that the simulated RFI measurement system measures burst RFI as expected by the SKA protocol.
8. If possible, check burst mode RFI measurements on the real RSA equipment.

The first objective is to be met by studying and comprehending the content of the SKA Memo 37, the RFI protocol. This will be done in Chapter 2 as part of the literature review. The second objective will be met by reviewing the relative material as documented by the SA RFI team, this will also be documented in the literature review. The specifications of the components of the proposed RFI measurement system 4 will be researched from the SA RFI team. From the specifications of the components as researched, the receiver will be simulated in SystemView. The simulated receiver will be investigated if it meets the protocol requirements. The burst mode systems operating in the L-band will be researched, simulated in SystemView and injected in the receiver. Since the RFI measurement system 4 has been built. It was desired to compare the practical system to the simulated receiver. Similar tests done on the simulated receiver will then be verified in the practical system. In essence, this will reveal if the simulated receiver replicates the practical system and measures RFI as required by the protocol.

1.2 Background to investigation

The SKA core array will have to be located in a remote area, that is, a radio interference-free area. Since the SKA is a radio telescope in nature, RFI measurements and reporting are therefore the first requirements for countries contending to host the SKA. The Independent Communications Authority of South Africa (ICASA) and Hartebeesthoek Radio Astronomy Observatory (HartRAO) staff, on behalf of the National Research Foundation (NRF) and the Department of Science and Technology (DST), conducted the initial RFI survey in South Africa for SKA sites. The proposed sites for the SKA in South Africa included the Kalahari Site (the name of the desert on which it is located), the Namaqualand Site (named after the Nama people who live there) and the Karoo Site (the large dry area which dominates the centre of the country) [1].

Although the preliminary measurements (in November 2003 and January 2004) were using conventional communications RFI instrumentation, the results were sufficient to demonstrate that the sites being observed were relatively quiet over the 150 to 3000 MHz frequency range. The equipment used for the survey lacked the sensitivity required for radio astronomy RFI surveys [5]. Therefore, the South African SKA Steering Committee decided to do a full test at the Kalahari site, which was found to be one of the quietest of the three sites in the earlier studies [5].

Based on the RFI protocol, the experience gained with the equipment used for preliminary RFI measurements, as well as the proposal from ASTRON[1] and comments from equipment suppliers, the RFI Measurement System 1 was proposed, designed and assembled [6]. This system is described in great detail in Chapter 2. The RFI measurement system 1 was deployed in December 2004 in order to satisfy the original RFI measurement deadline stipulated by the ISPO[2] [3]. The pressure to deploy the system and the relatively high RFI environment near the HartRAO workshops did not allow thorough investigations of self-generated signals radiated by the measurement set. The radio quiet environment at the site revealed a number of self-generated RFI that were not previously apparent [3].

Also, the RFI Measurement System 1 failed to meet the protocol requirements specified in Table 1 of the SKA Memo 37 in band 5 (L-band) because of the following reason. In Mode 1[3], a very short dwell time (2 micro-seconds) over a large 1 MHz bandwidth is required in the 960 MHz to 1400 MHz band (L-band). This is because this frequency band is allocated to aircraft navigation used by Distance Measuring Equipment (DME) and Secondary Surveillance Radars. The spectrum analyzer was not capable of scanning as fast as the specified 2 μs dwell time would require. As a compromise the fastest sweep time supported by the instrument was selected, and the sweep span was matched to the entire frequency span of band 5 [3]. Furthermore, the number of times this entire band

[1]The Netherlands group responsible for the SKA Site Spectrum Monitoring for all candidate sites.

[2]International SKA Project Office hosted by Astron.

[3]Mode 1 is a set of measurements where strong interferences are investigated using short dwell times and many repetitions.

is to be swept per measurement cycle as specified in the RFI protocol could not be met. This is because of the relatively slow sweep time of the spectrum analyzer. The number of repetitions, $N_{rep} = 18000$, for the L-band was chosen (instead of 10^6 required) to match the aggregate measurement time specified for this band in the Mode 1 measurements [3]. As an alternative to the use of the spectrum analyzer, it was proposed that an L-band dedicated FFT spectrometer be built from standard components, state of the art Field Programmable Gate Array (FPGA) board with a high speed 14 bit Analogue to Digital Converter (ADC). This thesis project investigates the option and the capability of such a system to correctly measure RFI as desired by the protocol. It must be noted however that the RFI measurement system 1 and its duplicates discussed in Chapter 2 were used in the final RFI measurements conducted in October 2005 due to deadline constraints. The proposed RFI measurement system 4 was built independently from this thesis, and was never used for RFI measurements in the bidding process. The problems investigated in this thesis project are listed below.

1.3 Problems to be investigated

The problems to be investigated in this thesis can be summarised as follows:

- Investigate the receiver design of the RFI measurement system 4.
- Investigate if the RFI measurement system 4 conforms to the protocol specifications in all respects and that it measures man-made radio frequency interference as required by the protocol.
- Investigate Distance Measuring Equipment interference in the 960 - 1400 MHz frequency band, with particular emphasis on the power levels they are likely to be detected at, and then check if they saturate the measurement system.

1.4 Limitations and Scope of the Study

This thesis project investigates the L-band RFI measurement system 4. Although the RSA RFI measurement systems cover the frequency band from 70 MHz to 26.5 GHz, the focus of the investigation is limited to the part of the RSA RFI measurement system that processes the L-band. This is because none of the existing RFI measurement systems could measure RFI as required by the protocol. The 1215 - 1400 MHz band is also very important to radio astronomers for spectroscopy of HI at high redshift, pulsar work and SETI [8].

1.5 Plan of Development

Chapter 2 presents the literature reviewed in this thesis project. In the context of this thesis project, literature review refers to the understanding of the electronics used in the assembly of the proposed RFI measurement system 4. The difference between the proposed system and the three systems used in the RFI measurements for the bid is briefly covered. The three systems are called the RFI measurement system 1, system 2 and system 3. System 1 and system 3 are similar, and are used for Mode 1 measurements. System 2 is similar to System 1 and 3, except for the extra low-noise gain block that is common to all signal paths and whose function is to defeat the spectrum analyzer contribution to the system noise temperature. System 2 is used for Mode 2 measurements at the core site only [3].

The chapter begins with a summary of the protocol key issues, followed by a review of the three RFI measurement systems, and finally a detailed review of the RF electronics used in the RFI measurement system 4.

Chapter 3 discusses the simulation of the receiver of the RFI measurement system 4, and the simulation of the DME signals found in the L-band. The receiver simulation is presented first, followed by the DME signals simulation. The simulated DME signals are injected in the receiver input as if they are the received signals. This means that the power level of the DME signals is calculated as the received power assuming the antenna gain of the RFI measurement system.

The receiver consists of what is called in this report, the receiver front-end (first RF stage) and the receiver back-end (FPGA demodulating electronics). The receiver front-end is made up of non-monolithic RF and Microwave components and the demodulator is a Field Programmable Gate Array. This chapter describes the simulation of these two receiver parts. The simulation of each component (LNA, cable, wide-band amplifier, switch, variable gain amplifier, mixer, local oscillator, baseband amplifier and filter) is thoroughly described. The filters employed in the in-phase and quadrature channels are also justified, followed by a description of the analogue to digital conversion.

The chapter ends with a discussion of the simulation of the Distance Measuring Equipment (DME) signals in the 962 - 1213 MHz range. The DME signals are researched here because they are expected with *very* high peak power and short duration and are suspected to give problems to the receiving system.

Chapter 4 presents the tests performed on the simulated receiver and the parameters that were calculated in order to characterise the receiver. The chapter begins with the basic theoretical calculations that are important in finding out the receiver's capabilities. For instance, the minimum and maximum detectable signal power.

The system gain is treated first, and the receiver is found to have a minimum and maximum gain due to the VGAs. The gain values are verified in the simulation tests by looking at the output power level of a known input signal power. Following that, is the vital noise

temperature of the receiver which must obey the protocol requirements. Using the noise figure calculator of the AppCAD from Agilent Technologies, as well as the SystemView simulation, the noise temperature of the receiver is computed. This is followed by the investigation of the dynamic range of the receiver. The receiver dynamic range is set by the minimum and maximum detectable signal power. The investigation of the power levels of these signals is carried out at maximum gain.

The maximum detectable signal power indicates the power level where harmonic distortion begins and inter-modulation products begin to show. This is also confirmed by feeding the receiver with signals larger in amplitude than the maximum detectable signal. This concept is further tested by tracing a small and a large amplitude signal in the receiver chain by means of a graph showing the signal amplitude at consecutive stages of the receiver, taking into account both the minimum and maximum gain of the VGAs.

The chapter ends with two-tone testing, where the power level of the two-tone signal that causes unacceptable inter-modulation products is investigated. Simple CW sinusoidal waveforms are used in the two-tone testing. The other tests that are performed use the simulated DME signals at various amplitude levels starting from -110 dBm and increasing in 5 dB steps.

It must be stressed that, since the simulated receiver could not be automated, the following tests assume manual mode. Also, only the minimum and maximum gain of the VGAs are considered in the tests unless otherwise stated.

Chapter 5 presents the practical tests that were done on the RFI measurement system 4. The purpose of the tests was to ensure that the simulated receiver replicates the practical system and to confirm the simulated receiver predictions. And most importantly, to investigate if DME-like signals are correctly measured by the system and do not saturate the receiver.

Because of the difficulty in injecting the signals at the LNA input or via the antenna, it was decided to perform the tests on the demodulator and the digitiser. However, the accumulated gain of the receiver front-end is accounted for in the signal processing. In other words, the RF signal is injected at the RF input of the demodulator where the signal from the antenna mast would normally be connected. The accumulated gain in the receiver front-end is then considered in signal processing to account for the full receiver chain gain. Otherwise, in practise the receiver back-end (demodulator and digitiser) is sufficient to demonstrate the receiver's capabilities. The terms "receiver" or "system 4 " are used in this chapter to refer to the receiver back-end being tested.

The receiver is tested using two types of RF signals: the continuous waveform (CW) sinusoidal signals, and amplitude modulated waveforms with DME signal characteristics. The tests using CW signals are presented first, followed by the amplitude modulated waveforms with DME signal characteristics. The tests using CW signals are done to demonstrate any difference in the way the receiver measures the CW signals to the DME signals.

The receiver has two modes of operation: (i) manual mode and (ii) Automatic Gain Control (AGC) mode. The manual mode is where the gain of the variable gain amplifiers is adjusted manually using a potentiometer. The receiver is tested for performance in both of these modes of operation. The receiver is tested using CW signals in both modes, whereas the DME-like signals are only tested in AGC mode. This is because, using CW signals it was found that manual mode, minimum gain, is not good for making measurements of this nature. In manual mode, only the minimum and maximum gain is considered as the power level of the RF signal is varied.

Chapter 6 documents the conclusions made from the study and presents the recommendations for better receiver performance, and particularly how to measure burst mode RFI in the L-band.

This research has confirmed that the receiver under investigation, the RFI measurement system 4, can and will measure DME RFI without suffering from compression and intermodulation distortion. Manual mode and maximum gain is the preferred choice for RFI measurements, but care must be taken for interference sources closer than 11.5 km as they will saturate the receiver. In this case, moderate gain will have to be used and the data calibrated accordingly. The measurement of RFI in AGC mode is forbidden since the gain of the AGC is unknown and thus calibration is impossible.

Chapter 2

Literature Review

This chapter presents the literature reviewed in this thesis project. In the context of this thesis project, literature review refers to the understanding of the electronics used in the assembly of the proposed RFI measurement system 4. The difference between the proposed system and the three systems used in the RFI measurements for the bid is briefly covered. The three systems are called the RFI measurement system 1, system 2 and system 3. System 1 and system 3 are similar, and are used for Mode 1 measurements. System 2 is similar to System 1 and 3, except for the extra low-noise gain block that is common to all signal paths and whose function is to defeat the spectrum analyzer contribution to the system noise temperature. System 2 is used for Mode 2 measurements at the core site only [3].

The chapter begins with a summary of the protocol key issues, followed by the review of the three RFI measurement systems and finally a detailed review of the RF electronics used in the RFI measurement system 4.

In Mode 1, the protocol [7] specifies a dwell time of 2 μs duration over a large 1 MHz bandwidth in the 960 -1400 MHz band (L-band). The reason for this short dwell time is to capture and characterize pulsed interference from radars and DME in this band. This kind of interference is expected, potentially with very high peak power [9]. Executing these measurements with the spectrum analyzer leads to very long measurement times approximated at 5.5 hours readout time per measurement cycle [9].

For this reason alone, the required time grows from the estimated 3.3 effective days to 13.1 days if a million repetitions are to be made ([9], page 11). To avoid the long measurement times, it was proposed to investigate the option of building a dedicated FFT spectrometer from standard components, state of the art FPGA board with a high speed 14 bit ADC. This proposed system was called system 4 and its design (electronics) forms basis of this chapter. The protocol requirements are reviewed next, followed by a description of the three RFI measurement systems.

2.1 RFI Measurement Protocol for SKA sites

The RFI measurement protocol is briefly discussed in this report because of the following two reasons:

1. It is the document from the which the designed systems are striving to conform to in terms of the instrumentation used, measurements requirements and site characterisation. Therefore any protocol requirements not met by these systems can be easily explained if the protocol is understood.

2. The proposed FFT spectrometer must comply to the protocol requirements in every aspects. Again, comprehending the protocol will ensure all of its specifications and requirements are catered for in the proposed RFI system 4.

The protocol spells out the instrumentation requirements, site characterization minimum requirements, and the RFI measurements requirements to be met. The purpose of the protocol is to establish a standard procedure for the measurement and reporting of RFI at any given site for use in the SKA site evaluation process [7]. The protocol seeks to identify RFI originating from terrestrial or airborne sources. Satellites and astrophysical sources of RFI are considered to be more or less the same for all candidate sites, and thus not of interest in this evaluation. For this reason the emphasis is on azimuthal coverage in the plane of the horizon [7].

The protocol divides the measurements into two parts, Mode 1 and Mode 2. *Mode 1*, with low sensitivity requirements, is defined for the observation of strong RFI and is relevant for SKA receiver linearity analysis [7]. *Mode 2*, with high sensitivity requirements, is defined for the observation of weak interferences, which potentially threatens to obscure weak signals of interest [7]. The instrumentation requirements and measurements requirements that are specified by the protocol for RFI measurements are summarised below.

2.1.1 Instrumentation Requirements

The complete instrumentation requirements are specified in the protocol [7], relevant to this project are the following:

- Discone antennas covering the band 70 MHz to 20 GHz. At least 3 antennas would be required to span this range. The suggested convenient choice is the log-periodic antennas for low frequencies and horn antennas at high frequencies. The frequency range was later extended from 60 MHz to 26.5 GHz.

- Receiver temperature $T_R \leq 3 \times 10^4$ K for *Mode 1* and $T_R \leq 300$ K for *Mode 2* measurements, defined for the purpose of the protocol to be measured at the antenna terminals back (not from the receiver or spectrum analyser input) and thus include low-noise amplifier (LNA), external filters, and cable losses.

2.1.2 Measurements Requirements

Table 1 in the SKA Memo 37 [7] provides the specifications for Mode 1 "measurement cycles" as determined by the Working Group on RFI Measurements and shown in Table 2.1. RBW stands for resolution bandwidth and is also the spacing between centre frequencies examined. *Dwell* is the length of time that a channel (one slice of spectrum having width equal to the specified RBW) is examined. *Reps* is the number of times the experiment should be repeated per iteration of the measurement cycle. $S_{0\mathrm{h}}$, is the expected flux density at zero-elevation (that is, along the horizon) for a signal matched in bandwidth that generates -100 dBm at the antenna terminals. The flux density defines the sensitivity of the instrument in each band if the specified parameters are utilised. A detailed description of this flux density can be found in the Appendix A of the protocol.

The specifications in Table 2.1 were translated by the S.A. RFI team into spectrum analyzer settings and schedule parameters for use by an automated measurement system ([3], page 23). It is essential to note that in the fifth frequency band in Table 2.1, a million repetitions over a large 1 MHz bandwidth in a dwell time of 2 μs per measurement cycle, are required.

Table 2.1: **Mode 1 Measurement Cycles.**

Frequency (GHz)	RBW (kHz)	S_{0h}dB(Jy)	Dwell (ms)	Reps	Total (s)
0.070 - 0.150	3	-166	10	5	1334
0.150 - 0.300	3	-159	10	1	500
0.300 - 0.800	30	-163	10	1	167
0.800 - 0.950	30	-155	10	20	1000
0.950 - 1.4	**1000**	**-168**	**0.002**	10^6	**900**
1.4 - 3	30	-150	10	1	534
3 - 20	1000	-158	10	1	170
TOTAL					4604

From the requirements stated in the SKA Memo 37, the South African RFI measurement systems 1, system 2 and system 3 were designed by Dr. George Nicolson[1] and assembled by the HartRAO technical staff. The three RFI measurement systems are briefly described next, followed by the key protocol issues encountered during the measurements.

2.2 The RFI Measurement Systems

The description of the RFI measurement systems is written here as extracted from ([3], Chapter 3), and is included in this report to give an understanding of the reasons behind the proposed system. All three RFI measurement systems were designed for fully automatic unattended operation in order to ensure data reliability and simplify logistical

[1] Dr. George Nicolson is an Emeritus astronomer at HartRAO and a special adviser of SKA/KAT South Africa.

considerations. The measurement systems are all mounted on road trailers and are completely self-contained and mobile. The road trailers support the mast, an air-conditioned cabin and a diesel generator. Table 2.2 lists the main components and sub-systems that comprise each measurement system.

Table 2.2: **List of major system components comprising an RFI measurement system.**

Item	Description
1	Custom built road trailer with air conditioned cabin
2	Yanmar YDG5001SE 5kW air-cooled diesel generator
3	Pneumatic telescopic mast with 12 volt compressor
4	Yaesu G-5500 azimuth and polarization rotator
5	Mast Head RF Assembly
6	R&S HL033 log-periodic low frequency antenna
7	R&S HL050 log-periodic high frequency antenna
8	Sucoflex coaxial cable and multi-core control cables
9	Equipment rack in cabin (unshielded but minimum RFI leakage)
10	Agilent spectrum analyzer mounted in a ventilated EMC enclosure
11	Control PC mounted in ventilated EMC enclosure
12	Control circuitry mounted in ventilated EMC enclosure
13	Laptop computer for system configuration, debugging and data downloading
14	complete set of tools

2.2.1 Mast Head Electronics

Figure 2.1 shows the layout of the electronics for measurement systems 1, 2 and 3. The extra low-noise 14 dB gain block only applies to system 2. Heterodyne down-conversion is used to reduce the frequency of signals coming down from the mast-head to the spectrum analyzer. The mast-head local oscillators are locked to the 10 MHz reference signal produced by the Agilent spectrum analyzer. Various RF switches select the antenna, LNA and mixer for the band being measured. The noise diode can be switched to any signal path to replace the antenna, hence allowing the measurement of receiver temperature T_{R} relative to the antenna terminals.

System 1 and 3 easily achieve the T_{R} <30000 K specification required for Mode 1 measurements. The additional gain block in system 2 ensures T_{R} <300 K for a wide frequency range, as required for Mode 2 measurements. System 2 is used for Mode 2 measurements only at the core site. System 1 and 3 are used for Mode 1 measurements at all SKA sites.

Two Rohde & Schwarz log-periodic antennas are employed by each RFI measurement system. The HL033 is used to cover the band from 70 MHz to 2 GHz, and the HL050 covers the 2 GHz to 26.5 GHz band. Both antennas are simultaneously mounted on the mast-head assembly, pointing in opposite directions. The smaller HL050 is mounted directly on the mast-head RF enclosure to ensure short cable runs, and the larger HL033 is mounted on a boom extending out of the opposite end of the enclosure.

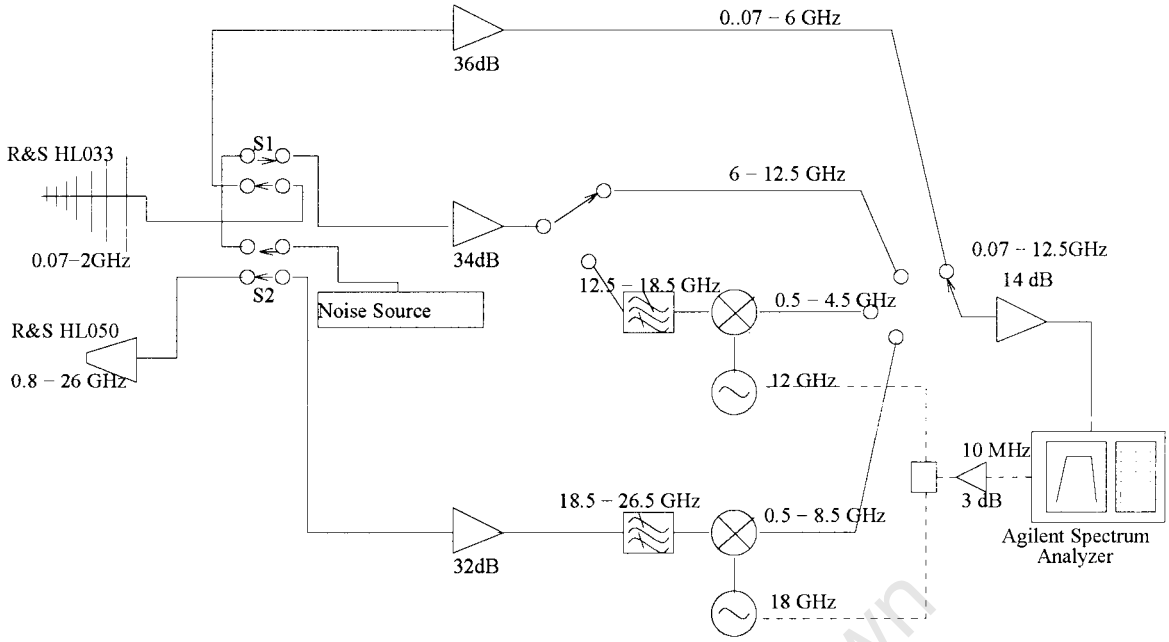

Figure 2.1: Block diagram of the RFI measurement system 1, system 2 and system 3. The extra low-noise 14 dB gain block only applies to system 2.

The mixers used are simple Double Side-Band (DSB) mixers, hence image rejection filters were required. The required waveguide high-pass filters were built in HartRAO. Chapter 3 of reference [3] shows the constructed image rejection waveguide filters as well as their frequency response graphs. The three RFI measurement systems were used by the SA RFI team for the South African SKA bid. However, the protocol specifications could not be met in the L-band using these measurement systems. The following section discusses the problems encountered and how they were solved.

2.3 Mode 1 Protocol Key Issues

From the above brief description of the protocol requirements, the RFI measurements were performed using the three systems, the following key issues were found by the S.A. RFI team:

1. The strategy for determining spectrum analyzer settings was not possible for band 5 in Table 2.1, because the spectrum analyzer was incapable of scanning as fast as the specified 2 μs dwell time would require. As a compromise the fastest sweep time supported by the instrument was selected, and the sweep span was matched to the entire frequency span of band 5 [3].

2. The specified 10^6 number of times the entire band must be swept, per measurement cycle, proved impractical because of the relatively slow sweep time of the spectrum analyzer.

It was therefore proposed that this band be processed by an FFT spectrometer. The proposed RFI measurement system 4 was design and built by Dr. Adrian Tiplady[2]. The system uses the AD8347 direct quadrature demodulator to down-convert RF signals to baseband. The AD8347 is an integrated circuit that performs direct conversion quadrature demodulation. The chip is a product of Analog Devices hence the name "AD". The complex signal from the AD8347 is then low-pass filtered by two filters (one for each channel) with a total bandwidth of 100 MHz. The baseband In-phase and Quadrature signals are then fed into a PCM 480 dual channel digitiser card, that samples the two channels at 105 MSPS. Finally a purpose written software performs the FFT on the sampled data and produce a plot of the power level (in dBm) of the signal versus the frequency over a 100 MHz bandwidth, extending from -50 MHz to 50 MHz. The proposed RFI measurement system 4 is discussed next.

2.4 RFI Measurement System 4

2.4.1 Receiver Front-end

The schematic diagram of the L-band receiver **front-end** of *System 4,* implemented by the SA RFI team, is shown in Figure 2.2 below. The signal is received by a linear polarised directional antenna covering the 80 MHz to 2 GHz band, product of Rohde & Schwarz, with a gain of 6.5 dBi. The 6.5 dBi means the antenna gains is 6.5 decibels more than the isotropic radiator gain of 0 dB.

The Agilent 346C noise source contaminates the signal from the antenna with noise via a Narda Microwave Group switch. The noise source is used to compute the noise temperature of the system in a method called the Y-factor method ([12], Page 88). This means the noise diode is generally switched off unless calibration is taking place.

The signal is then passed to the Miteq^{R} LNA. The signal from the LNA is switched to a 14 dB wide-band amplifier and then switched to the FPGA where quadrature demodulation takes place. The cables connecting the RF and Microwave components in the system have losses as shown by Ls below. The quadrature demodulator is discussed next.

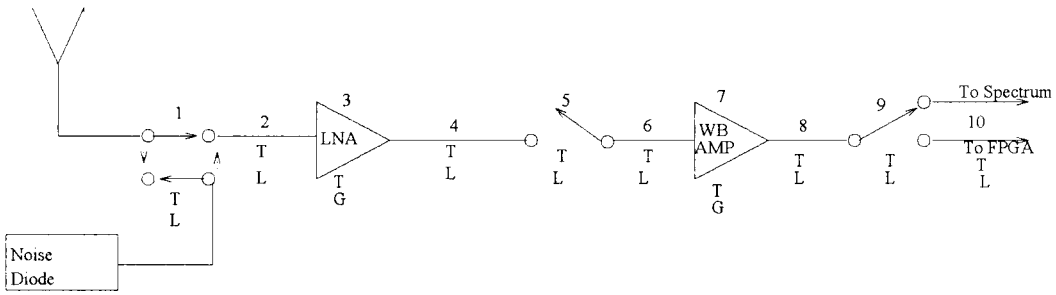

Figure 2.2: Receiver front-end of the RFI Measurement system 4.

[2]Dr. Adrian Tiplady is an assistant project scientist in the South African SKA team.

2.4.2 Receiver Back-end

The AD8347 Quadrature Demodulator is a programmable chip as shown in Figure 2.3. The demodulator RF and LO inputs connectors are located in the printed circuit board. The RF input is ac-coupled to ground using 100 pF capacitors. The LO input is transformed into a differential input by a very small transformer. The LO inputs are differentially driven for optimum performance [14]. A 200 Ω shunt resistor is placed between the two differential LO signals to improve the match to a 50 Ω source [14]. The differential outputs of the transformer are fed into LOIN and LOIP of the AD8347 (*see* Appendix A).

Demodulation of the RF signals is performed by mixing the RF signals with the LO signals. The RF signal is split into two in-phase signals (after some amplification) and then fed into two mixers which down-converts the RF signal to baseband using two differential LO signals (that are 90^0 out of phase to each other). The resulting baseband output signals of the AD8347 are the In-phase and the Quadrature signals, from a differential baseband amplifier. Therefore the In-phase and the Quadrature outputs are differential outputs. The data sheet of the AD8347 is included in Appendix A.

The In-phase and the Quadrature differential outputs are fed into two (one for each channel) AD8130 buffer amplifiers of unity gain which transform their differential input into single-ended outputs. The AD8130 is a differential-to-single-ended converter that operates up to 270 MHz.

The signals from the AD8130 amplifiers are low-pass filtered. The two silver rectangular blocks on the bottom-right of Figure 2.3 are low-pass filters with a 3 dB cut-off frequency of 55 MHz.

The filtered In-phase (I) and Quadrature (Q) output signals are then fed into a PCM 480 dual channel digitiser card, with two 14 bit Analogue to Digital converters that samples the two channels at 105 MSPS. Two RF cables of equal lengths transport the two filtered outputs into the PCM 480 digitiser card shown in Figure 2.4. The digitizer sampled data is then routed to the Matlab program that does the FFT. Briefly, the data from the two channels is combined to form a complex signal. Then FFT processing takes place where the power spectrum is the final plot. The purpose written program can do either 128 or 512 FFT.

The AD8347 demodulator can operate in either automatic mode or manual mode. Notice that a potentiometer is available for manual mode operation. The potentiometer is used to adjust the gain of the AD8347 demodulator during manual mode.

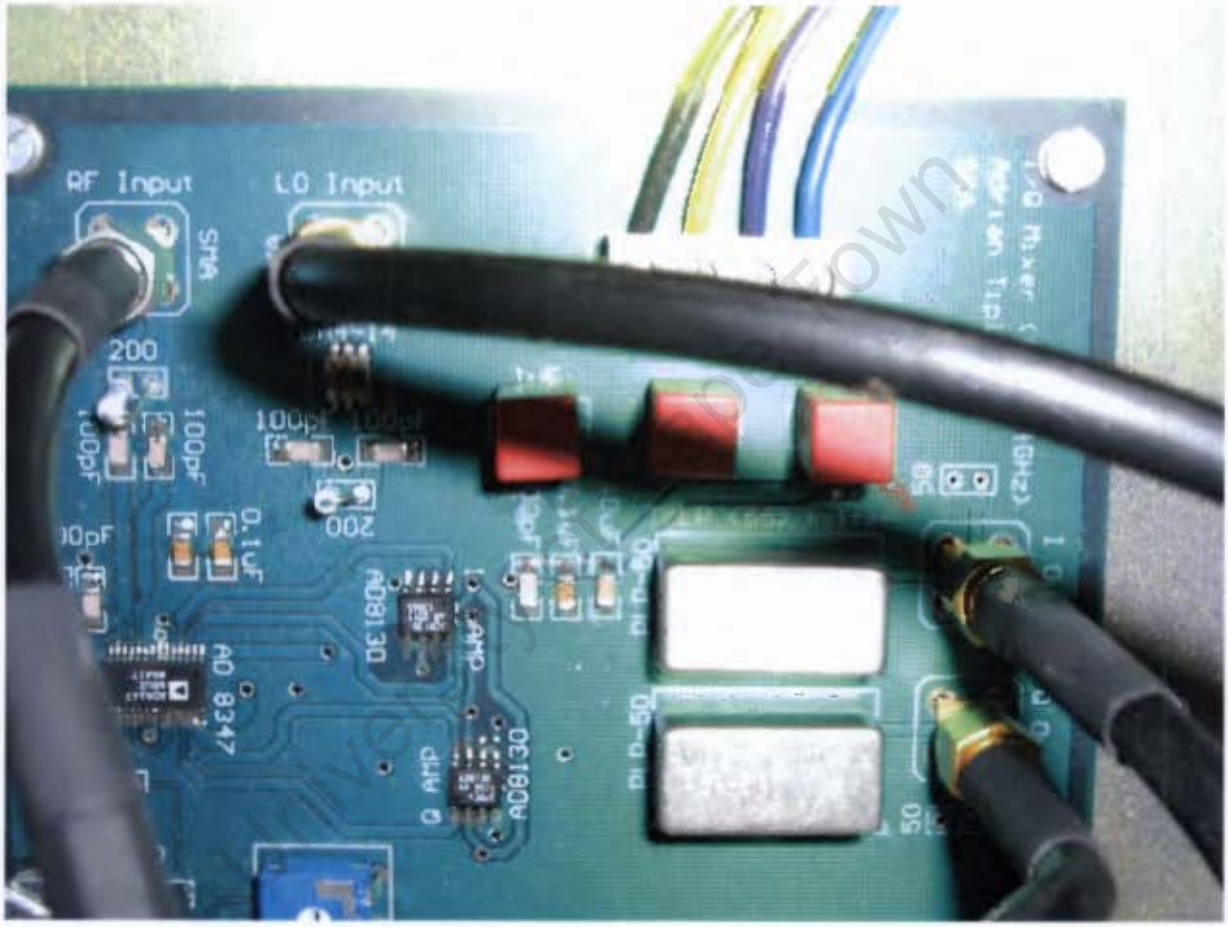

Figure 2.3: Picture of the PCB depicting the AD8347 quadrature demodulator, the AD8130 unity gain buffer amplifiers, and the RF and LO SMA input connections.

Figure 2.4: The rear of a computer showing the PCM 480 card with the In-phase and Quadrature connections from the demodulator.

2.4.3 AD8347 Theory of Operation

Figure 2.5 shows the schematic diagram of the AD8347. The AD8347 is a broadband Direct I/Q Demodulator with RF and baseband (IF) Automatic Gain Control (AGC) amplifiers. An RF signal in the frequency range of 800 MHz to 2700 MHz is directly down-converted to the I and Q components at baseband using a local oscillator (LO) signal at a frequency 10 MHz below the RF signal [14].

The RF input signal goes through two stages of Variable Gain Amplifiers (VGAs) before splitting up to reach two Gilbert-cell mixers. The mixers are driven by a pair of LO signals which are in quadrature. The outputs of the mixers are applied to baseband I and Q channel variable gain amplifiers. The outputs from these baseband variable gain amplifiers are then applied to a pair of on-chip, fixed gain, baseband amplifiers. These amplifiers gain up the output signal by 30 dB to a level compatible with most A-to-D converters. The RF and baseband amplifiers provide approximately 69.5 dB of gain control range [14].

Local Oscillators (LO)

The Local Oscillator (LO) quadrature phase splitter employs polyphase filters to achieve high quadrature accuracy and amplitude balance over the entire operating frequency range.

The polyphase phase splitters are RC networks connected in a cyclical manner to achieve gain balance and phase quadrature ([14], page 16). For optimum performance, the LO is driven differentially. A LO drive level of -8 dBm is recommended (*[14], Page 18*). Although a single-ended drive is possible, it slightly increases the LO leakage. In the RFI measurement system 4, the LO is differentially driven (see Figure 2.2).

Variable Gain Amplifiers (VGAs)

The VGAs have a gain range of 69.5 dB, where the minimum conversion gain is -30 dB and the maximum conversion gain is 39.5 dB. The minimum conversion gain occurs when the gain control voltage is 1.2 V, and maximum conversion gain occurs when the gain control voltage is 0.2 V. This means that the gain control function has a negative sense, increasing the control voltage decreases the gain. In Figure 2.5, RF AMP1, RF AMP2, and IF AMP1 (together with mixer) yield this 69.5 dB gain range mentioned above. This means that the maximum gain at points X and Y is 39.5 dB. IF AMP2 has a gain of 30 dB which totals the demodulator gain to 69.5 dB [14].

Mixers

Two double-balanced Gilbert-cell mixers, one for each channel, perform the in-phase and quadrature down-conversion. Under Automatic Gain Control (AGC), the maximum allowable mixer output power level is -6.5 dBm (600 mV peak-to-peak into 200 Ω) [14]. In practise, under AGC mode, to ensure that the maximum allowable mixer output power level is not exceeded, the mixer output pins are connected to an on-board sum of squares detectors. The inputs to this rms detector are referenced to VREF, the reference voltage. *Any difference between the mixer output level and VREF forces a compensating voltage onto the mixer output* [14]. The time constant of this correction loop is set by the capacitors that are connected to the I and Q channel offset nulling points. For normal operation, 0.1 μF capacitors are recommended. The summed detector output drives an internal integrator which, in turn, delivers a gain correction voltage to the VAGC pin, the Automatic Gain Control Voltage pin. A 0.1 μF capacitor from VGAC to ground sets the dominant pole of the integrator circuit [14]. The corner frequency of the compensation loop is approximately given by:

$$f_{3\text{dB}} = \frac{40}{C_{\text{OFS}}}(C_{\text{OFS}}\text{in}\mu\text{F}) \tag{2.1}$$

where C_{OFS} is the value of the offset nulling capacitor [14]. Therefore the corner frequency of the compensation loop is:

$$f_{3\text{dB}} = 400\ \text{Hz}$$

Therefore, the period of the compensation loop is 2500 μs. This is how long it takes to do

gain correction. The corner frequency of the compensation loop is set to be much lower than the symbol rate of the demodulated data in order to prevent the loop from falsely interpreting the data stream as a changing offset value. The theory of operation of the AGC can be found in reference .The mixer conversion loss is estimated at 6 dB, more on this in Chapter 3.

Output Amplifiers

The output amplifiers gain up the signal from baseband VGAs by 30 dB. The outputs of these amplifiers are differential. This is the output of the AD8347. This complex output is fed into two (one for each channel) AD8310 buffer amplifiers which convert the inputs into single-ended outputs. The buffer amplifiers have a gain of 0 dB. The single-ended outputs are filtered and then sampled as described above.

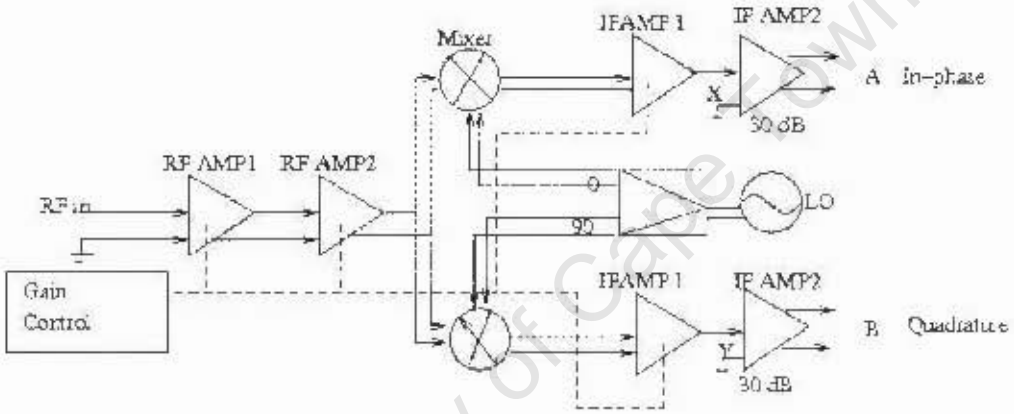

Figure 2.5: Block diagram of the actual Direct Conversion Quadrature Demodulator AD8347.

The L-band receiver front-end of Figure 2.2 and the quadrature demodulator shown in Figure 2.5 above are simulated in SystemView. The SystemView amplifiers used, are single-ended, therefore the buffer amplifiers are not simulated. The low-pass filters are also included in the simulation. The simulation is discussed in Chapter 3.

2.5 Summary

This chapter has presented the literature that is applicable in the thesis project. The chapter began with a discussion of the RFI measurement protocol requirements as found in the SKA Memo 37, with particular emphasis on the instrumentation requirements and Mode 1 measurement cycles requirements. The requirements for Mode 1 measurements in the L-band were noted to be a million repetitions per iteration of the measurement cycle, in a dwell time of 2 micro-seconds over a large 1 MHz bandwidth. The three RFI measurements sets used by the SA RFI team were then discussed. These three systems were found not to meet the protocol specifications in the L-band for Mode 1 measurements.

The manner in which this problem was solved during measurements was then discussed. The chapter ended with a discussion of the RFI measurements system 4, which was built to address the problems encountered in the L-band by system 1, 2 and 3. System 4 uses an FFT spectrometer to measure RFI in the L-band. The receiver of system 4 and its theory of operation were also presented. The next chapter discusses the simulation of the RFI measurement system 4 discussed above.

Chapter 3

L-band RFI Measurement System Simulation

3.1 Introduction

This chapter discusses the simulation of the receiver of the RFI measurement system 4, and the simulation of the DME signals found in the L-band. The receiver simulation is presented first, followed by the DME signals simulation. The simulated DME signals are injected in the receiver input as if they are the received signals. This means that the power level of the DME signals is calculated as the received power assuming the antenna gain of the RFI measurement system.

The receiver consists of what is called in this report, the receiver front-end (first RF stage) and the receiver back-end (FPGA demodulating electronics). The receiver front-end is made up of non-monolithic RF and Microwave components and the demodulator is a Field Programmable Gate Array. This chapter describes the simulation of these two receiver parts. The simulation of each component (LNA, cable, wide-band amplifier, switch, variable gain amplifier, mixer, local oscillator, baseband amplifier and filter) is thoroughly described. The filters employed in the in-phase and quadrature channels are also justified, followed by a description of the analogue to digital conversion.

The chapter ends with a discussion of the simulation of the Distance Measuring Equipment (DME) signals in the 962 - 1213 MHz range. The DME signals are researched here because they are expected with *very* high peak power and short duration and are suspected to give problems to the receiving system.

3.2 Receiver Simulation

The simulation of the receiver was done in SystemView. Figure 3.1 is the block diagram of the simulated receiver. In Figure 3.1, the simulated DME signal is injected at the LNA input not at the antenna. This is because the power level of the simulated DME signal,

already takes into account the gain of the antenna.

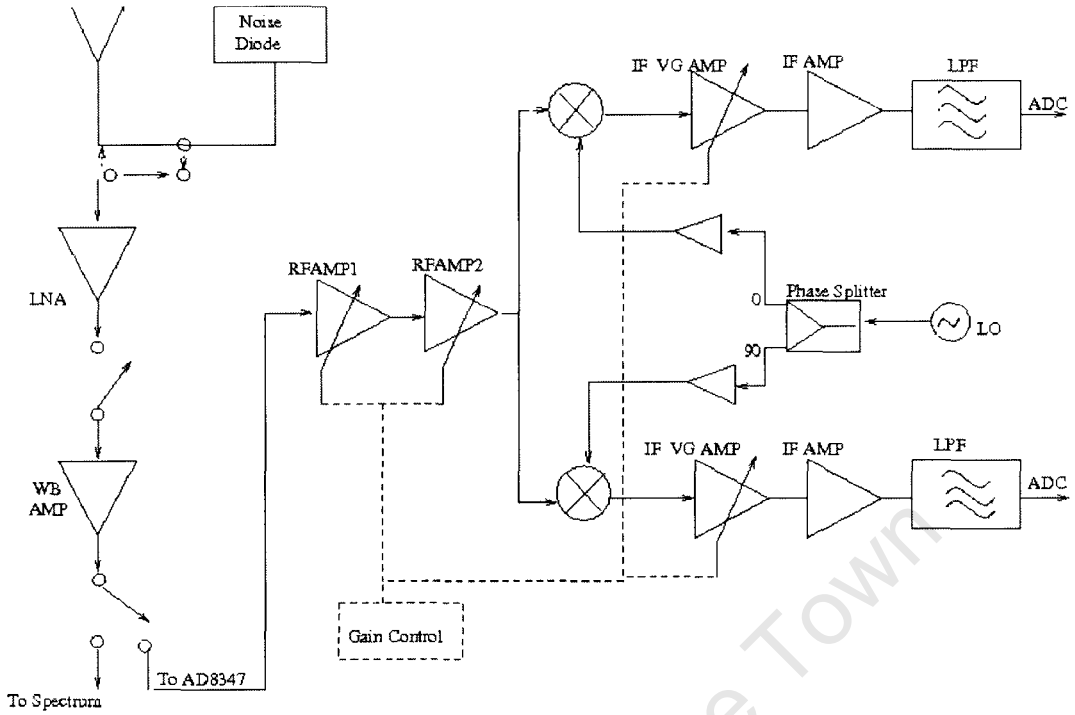

Figure 3.1: System level block diagram of the simulated receiver.

System 4 uses a quadrature demodulator shown on the right-hand side of Figure 3.1 instead of a spectrum analyzer. The simulated demodulator down-converts to an Intermediate Frequency (IF) of 10 MHz. The IF signals are sampled, and the sampled data out of the two channels (In-phase and Quadrature) is then used for FFT processing. The specifications of the demodulator are obtained from Analog Devices [14]. Because the AD8347 quadrature demodulator is a monolithic integrated circuit (IC) chip, the parameters of some of the components inside the chip could not be found even from the manufacturer. After a very exhaustive study of the specifications as found in [14] (page 3), the demodulator was simulated as explained in Sub-section 3.3.4 below. It must be emphasised that the low-pass filters are not part of the demodulator. The filters are on the printed circuit board, and the simulated filters are justified in Sub-section 3.3.5. The simulated receiver components specifications are obtained from their respective manufacturers and documented below.

3.3 Simulated Receiver Parameters

3.3.1 Cables and Switches

All cables and switches attenuate the signal by an amount as specified by their respective manufacturer and introduce noise in the system equivalent to the loss of the attenuator. The cables and switches are therefore simulated using SystemView's attenuator tokens,

with noise enabled. "Noise enabled" means that the token attenuates the signal by an amount, L(dB), and the attenuator has a noise figure F = +L (dB), where L is the loss of the lossy element in decibels. There are three Narda switches in the receiver front-end with losses 0.4 dB, 0.3 dB, and 0.3 dB respectively. Connecting components together in the receiver front-end are four RF cables with losses 0.3 dB, 0.2 dB, 0.3 dB, and 0.3 dB respectively.

3.3.2 The Low Noise Amplifier

The LNA is a product of Miteq whose product number is AFS4-00100600-13-10P-4. The LNA is simulated according to the real data specifications from the manufacturer [16]. The LNA specifications are summarised in Table 3.1 below. The specifications are simply entered into the SystemView amplifier token. The *third-order intercept point* P_3 of the LNA is **not** specified by the manufacturer. The approximate rule that many practical components follow is that, P_3 is 12 to 15 dB greater than P_1 (the *1dB compression point*) assuming these powers are referred to the same point ([12], pg 101, last paragraph). This approximate rule is applied in simulating the third-order intercept point of the LNA, $P_3 = P_1 + 12$ dB is used in the simulation.

Table 3.1: **Miteq LNA specifications used.**

Frequency (GHz)	0.1 - 6 GHz
Gain (dB)	36
Gain Flatness(±dB Max)	1.25
NF (dB)	1.3
VSWR(in/out)	2:1
P_{out} @1dBGCP	10 dBm
P_3 output	22 dBm

3.3.3 The Wide-band Amplifier

The wide-band amplifier is a product of Miteq whose product number is AFS2-00001200-25-8P-2. The wide-band amplifier is simulated according to its real specifications from the manufacturer's data sheet [16]. The specifications are summarised in Table 3.2. The same rule applied in the LNA 3rd-order intercept point is applied in the simulation of the wide-band amplifier's third-order intercept point. The wide-band amplifier is the last active component in the receiver front-end before the quadrature demodulator (other than the Narda switch). The RF signal from the wide-band amplifier is fed into the printed circuit board where the AD8347 Quadrature Demodulator is located. The AD8347 simulation is discussed next.

Table 3.2: **Miteq Wide-band Amplifier Specifications**

Frequency (GHz)	0.1 - 12 GHz
Gain (dB)	14
Gain Flatness(±dB Max)	1.25
NF (dB)	2.5
VSWR(in/out)	2:1
P_{out} @1dBGCP	8 dBm
P_3 output	20 dBm

3.3.4 AD8347 Quadrature Demodulator

It is essential to bear in mind that the following discussion focuses on one channel of the quadrature demodulator, and automatically applies to the other. In practise, under Automatic Gain Control (AGC), the mixer output is connected to a detector, whose output drives an internal integrator which, in turn, delivers a gain correction voltage to the AGC Voltage pin ([14], page 19). The mixer output has a maximum current limit of about 1.5 mA. This allows for a maximum allowable level at the mixer output of 600 mV p-p swing into a 200 Ω load ([14], page 6), that is -6.5 dBm. This corresponds to an RF input power level of -40 dBm at maximum gain of 39.5 dB [14]. This means that the mixer conversion loss is 6 dB, that is, the maximum allowable mixer power:

$$P_{\text{mixer-out}} = P_{\text{RFin}} + G_{\text{vga-max}} - L_c = -40 \text{ dBm} + 39.5 \text{ dB} - 6 \text{ dB} = -6.5 \text{ dBm}$$

where $G_{\text{vga-max}}$ is the maximum gain of the VGAs, and L_c is the mixer conversion loss. The manufacturer recommends a mixer local oscillator (LO) power of -8 dBm. The LO leakage power at the RF port is -60 dBm, and the LO leakage power at the IF port is -42 dBm [14]. The other mixer parameters are simulated from values estimated in the graphs in ([14], Page 13). The compression point of the mixer referred to the input is 16 dBm [14]. The noise figure of the demodulator is 11 dB at maximum gain. Since the mixer already contributes 6 decibels of this noise, it is apparent that the amplifiers share the other 5 dB. The low noise figure of the VGAs comes at no surprise because the AD8347 is a direct conversion quadrature demodulator intended for use as a receiver in communication systems like cellular base station, radio links and satellite modems. Therefore the first amplifiers must have low noise figures for better performance.

Figure 3.1 shows the simulated demodulator block diagram. RF AMP1, RF AMP2 and IF AMP1 have a gain range of 69.5 dB as in the real system, only that the simulated demodulator does not have the option for automation. However, since the power level of the incoming RF signal is known in the simulation, calculations can be made such that the mixer output power does not exceed -6.5 dBm. This means that the gain values are manually entered into SystemView. These gain values depend on the RF signal power. For nominal power levels not threatening to saturate the receiver, the maximum gain is used.

The gain is decreased as the RF signal power increases to detrimental levels. Therefore in a sense, the simulation replicates the practical system, with automation being the major difference.

The specifications of the AD8347 quadrature demodulator are given in [14] and documented in Table 3.3, Table 3.4 and Table 3.5. For the RF and IF VGAs, the third-order intercept point output values in Table 3.3 and Table 3.4, are calculated from the approximate rule used for the LNA and wide-band amplifier. The second-order intercept points are obtained from the data sheet. For the baseband fixed gain amplifier, the 1 dB compression point and the third-order intercept point are estimated from their respective graphs in the specifications ([14], Figure 23/24) at a baseband frequency of 10 MHz. The graphs values are given in dB Vrms, then converted to dBm by adding 13.01 dB.

Table 3.3: **The RF VGA amplifiers specifications**

COMPONENT	PARAMETER	Value
RF VGA	Gain Range	46 dB
	Max Gain	26 dB
	Min Gain	-20 dB
	2nd order Intercept	-4.5dBm or 65 dBm
	P_3 output@min or max Gain	-18.5 dBm or 51 dBm
	P_1 output @min or max Gain	-32dBm or 9.5 dBm
	Noise Figure @max Gain	2.5 dB

Table 3.4: **The IF VGA amplifiers specifications**

COMPONENT	PARAMETER	Value
RF VGA	Gain Range	23.5 dB
	Max Gain	19.5 dB
	Min Gain	-4 dB
	2nd order Intercept	-4.5dBm or 65 dBm
	P_3 output@min or max Gain	-18.5 dBm or 51 dBm
	P_1 output @min or max Gain	-32dBm or 9.5 dBm
	Noise Figure @max Gain	1.5 dB

Table 3.5: **The baseband amplifiers specifications**

COMPONENT	PARAMETER	Value
Baseband AMP	Fixed Gain	30 dB
	Noise Figure	1.5 dB
	Bandwidth	65 MHz
	2nd order Intercept	-49 dBc
	P_3 output@max Gain	20 dBm
	P_1 output @max Gain	13 dBm
	Noise Figure @max Gain	1.5 dB

3.3.5 Low-Pass Filters

In reference [14] page 21, the filter design considerations are given for the practical case. Filtering can be conveniently done at the IF VGA amplifier output (mixer output) and the baseband amplifier output can then be directly fed into an ADC. The practical system 4 however opted for filtering at the final demodulator output. The considered fourth-order low-pass filter has a 3 dB cut-off frequency of 50 MHz. The simulated receiver down-converts to an IF of 10 MHz. The filters employed in both channels are fourth-order Butterworth low-pass Infinite Impulse Response (IIR) filters with a 3 dB cut-off frequency of 50 MHz. The total baseband bandwidth is 100 MHz. The digitization of the complex signal is performed by a 14 bit Analogue to digital converter at 105 MSPS. This is simulated by a quantiser in SystemView, which has the same function as the real analogue to digital converter, except it does not need an external clock signal for synchronisation. The sampling is explained below.

3.3.6 Analogue to Digital Conversion

The simulated receiver measures RFI in the 960 - 1400 MHz frequency band (but the demodulator can operate from 800 MHz to 2.7 GHz). The maximum frequency in the 960 to 1400 MHz frequency band, is 1400 MHz, thus the sample rate of the simulation, $f_s > 2f_{\text{max}}$, must be twice the maximum frequency by Nyquist's criterion. To accommodate high-order products of the incoming signal, a system sampling frequency of 5 GHz was chosen. The simulation run time or stop time was set at 24 μs to allow the entire DME pulse pair to the transmitted as will be explained in DME simulation below.

However, the simulated ADC samples at $f_{\text{ADC}} = 105$ MHz, implying a sampling period, $T_{\text{ADC}} = 1 \times 10^{-8}$s for the ADC, thus the samples are T_{ADC} seconds apart. Because the sample rate of the simulated system is $f_s = 5$ GHz, but the ADC sampling frequency f_{ADC} is 105 MHz, this means a re-sampler at f_{ADC}, must precede the ADC input. Therefore a re-sampler at 105 MHz is employed before the ADC (quantiser). A decimator can also be used to yield the same ADC sampling frequency of 105 MHz. The re-sampler still satisfies the Nyquist criterion for the baseband signal at 10 MHz. The output of the digitiser is saved in a SystemView text file and imported into Matlab for later signal processing. A 14 bit quantiser with a 2 Volts voltage span is used in SystemView for this operation.

A quantiser is chosen in the simulation for its easy of use. The SystemView ADC requires a clock signal for synchronisation. Also, the ADC requires many text files (depending on the number of bits) per channel to store each bit in binary format. For instance, one 14 bit ADC will require 16 text files to store the bit stream. The quantiser on the contrary performs the same function as the ADC without any clock signal, and requires only one text file per quantiser output. The subsequent section discusses the simulation of the DME signal.

3.4 DME Signal Simulation

Two systems of interest are known to be operational in the L-band, namely: the Secondary Surveillance Radars (SSR) at 1030 MHz (ground-to-air interrogation) and 1090 MHz (air-to-ground response) and Distance Measuring Equipments (DME) in the 962 - 1213 MHz range. The primary surveillance radars are being phased out of civilian use in South Africa in favour of SSR and are therefore not of concern ([11], Chapter 2, page 40). The use of DME systems will continue nonetheless.

The DME signals are researched here because they are expected with *very* high peak power and short duration and are suspected to saturate the receiving system. The full theory of operation of DME is documented in Appendix B.

3.4.1 DME Signal Characteristics

According to the research done by Fisher [9] at the National Radio Astronomy Observatory using the Green Bank Telescope, as well as DME equipment suppliers, the DME pulses are approximately Gaussian in shape as a function of time, with a half-amplitude full-width of 3.5 micro-seconds. The DME pulse is approximated by the following equation as found in [9]:

$$V(t) \; \alpha \; e^{-0.5(t/\sigma)^2} = e^{-2.7726(t/W)^2} \tag{3.1}$$

where t is time, and W is the full-width half-maximum pulse width in the same units as t.

The research done by Fisher [9] further reveals that the peak power from a DME transmitter on a large jet aircraft is 300 Watts. However, smaller aircrafts use peak power on the order of 50 Watts and ground transmitters have peak power between 100 and 1000 Watts depending on the station's intended service. Manufacturers of aircraft transceiver claim a useful range of 550 km for a DME transmitter with a peak power of 300 W [9], but aircraft altitude and the separations between ground stations on the same frequency will often limit the range to less than 300 km.

It is reasonable to assume that at 250 km (slant range), the received power is most likely the smallest possible receivable power from the aircraft's transmitter. The highest receivable power being the one when the DME transmitter is closest to the receiving system. The antenna of the RSA RFI measurement system for the L-band has a gain of 6.5 dBi. Therefore, for the worst case scenario, λ equals 260.7 mm (1150 MHz) and the slant distance R equals 250 km, the received power by the RFI measurement system's antenna (neglecting atmospheric refraction, and assuming the main beam to be facing the transmitter) is estimated at:

$$P_{r-\text{smallest}}\,[\text{dBm}] = P_t\,[\text{dBm}] + G_t\,[\text{dB}] + G_r\,[\text{dB}] - 10\log(\frac{4\pi R}{\lambda})^2 \tag{3.2}$$

$$= 49.42 \text{ dBm} + 0 \text{ dB} + 6.5 \text{ dB} - 141.62 \text{ dB}$$
$$= -85.7 \text{ dBm}$$

assuming the aircraft is 35 000 feet above sea level and the transmitting antenna gain is 0 dB. The transmitter power is obtained as the average power of the transmitter as:

$$P_{\text{avg}} = 300 * \frac{3.5}{12} = 87.5\,\text{W} = 49.42\,\text{dBm} \tag{3.3}$$

taking into account that the pulse width is 3.5 μs and the pulse period is 12 μs. With this useful insight of DME characteristics, the DME pulse pair is simulated as follows.

3.4.2 DME Pulse Pair Simulation

Using two SystemView's custom-source tokens, two baseband Gaussian shaped pulses were produced, with a pulse width of 3.5 μs and the pulse period of 12 μs. The second pulse is shifted by 12 μs in the time domain. The two pulses are then added together producing a pulse pair that repeats after 12 μs with a total run time of 24 μs. The pulse pair is then modulated with a sinusoid at a DME transmitter frequency f_{DME} in the range 1025 to 1150 MHz. The output of the modulator is a high frequency Gaussian shaped pulse-pair with all the DME characteristics defined above. The simulated power level of the DME signal, differs depending on the scenario being simulated and the transmitter frequency chosen. The power level of the signal is calculated using equation 5.1. Figure 3.2 shows the simulated DME pulse pair in SystemView. The sine wave is enclosed in the Gaussian envelope and very high in frequency, hence the dark Gaussian shape. The frequency of the sine wave in Figure 3.2 is 1025 MHz, and the power level is -87 dBm which corresponds to 14 micro-Volts zero to peak.

The simulated DME pulse-pair is fed into the receiver low-noise amplifier input as if it were the received signal. The simulated receiver is then tested for saturation and inter-modulation distortion and the simulation performance is compared to the practical system. The simulation tests are documented in Chapter 4 followed by the practical tests in Chapter 5.

3.5 Summary

The simulation of the proposed L-band RFI measurement receiver can be summarised as follows. The injected DME signals set the simulation stop time to 24 μs. The system simulation sampling frequency is 5 GHz to satisfy the Nyquist criterion and accommodate products resulting from demodulating the input signals. The LNA, wide-band amplifier and the Quadrature demodulator electronic components are simulated according to their specifications as obtained from their respective manufacturers. Other components are simulated from parameters derived from either the relevant theory, or the rule of thumb,

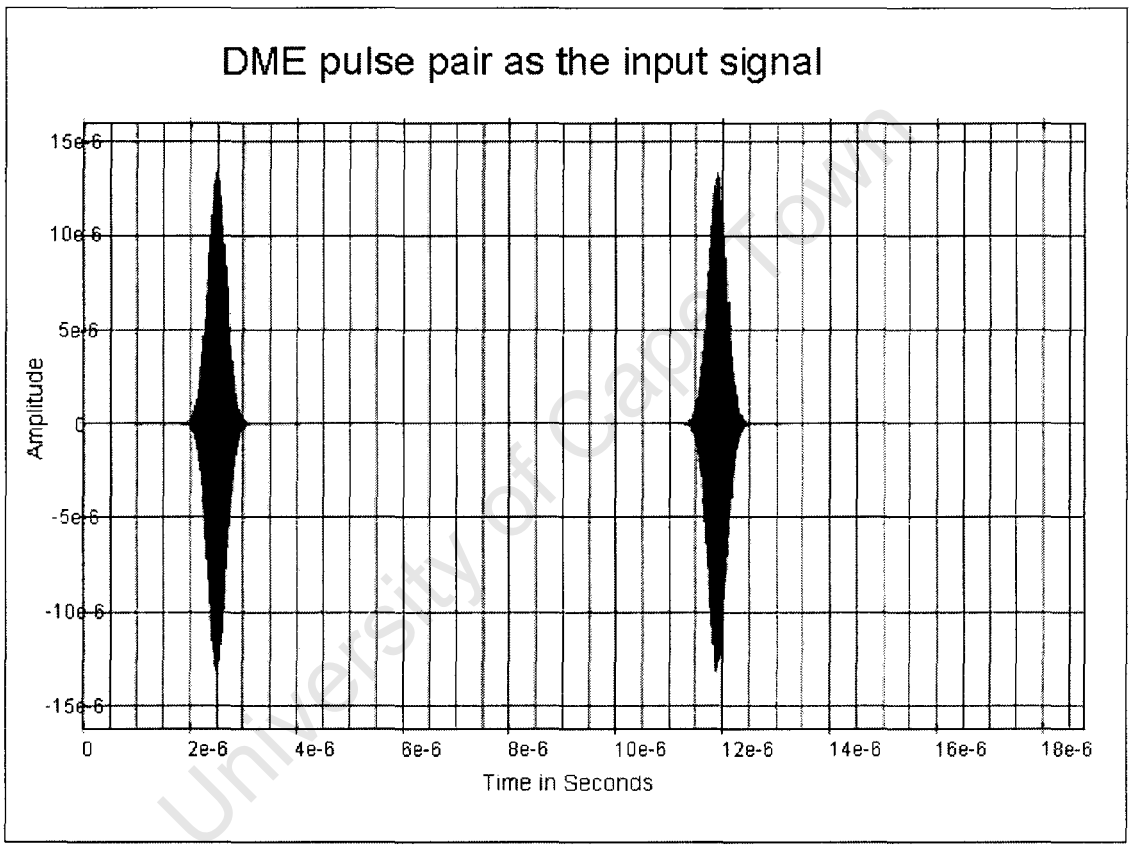

Figure 3.2: Simulated DME pulse pair.

or a well justified logic. For instance, the *third-order intercept point* P_3 of the LNA is **not** specified by the manufacturer. According to Pozar ([12], pg 101, last paragraph) many practical components follow the approximate rule that P_3 is 12 to 15 dB greater than P_1 (the *1dB compression point*), assuming these powers are referred to the same point. This approximate rule is applied in simulating in all the 3rd-order intercept points, $P_3 = P_1 + 12$ dB used in the simulation. Cables and switches attenuate the signal by fractions of a decibel, and are therefore simulated using SV attenuators with appropriate attenuation values.

The DME signals are simulated based on their characteristics as derived from reference [9]. The power level of the DME signals is calculated according to the scenario being simulated. The different scenarios assume different positions of the aircraft relative to the receiving system. The DME signals are the input to the receiver. The simulated receiver demodulates the DME signals into the in-phase and the quadrature using a local oscillator with an input power of -8 dBm. The complex baseband signal is at 10 MHz with a total bandwidth of 100 MHz. Two quantisers (*simulating* Analogue to Digital converters) sample the two channels. The sampled data is saved into text files and exported into Matlab for FFT processing. A plot of the signal magnitude in dBm versus the frequency in MHz is produced using Matlab as will be shown in Chapter 4.

Chapter 4

Simulation Tests

4.1 Introduction

This chapter presents the tests performed on the simulated receiver and the parameters that were calculated in order to characterize the receiver. The chapter begins with the basic theoretical calculations that are important in finding out the receiver's capabilities. For instance, the minimum and maximum detectable signal power.

The system gain is treated first, and the receiver is found to have a minimum and maximum gain due to the VGAs. The gain values are verified in the simulation tests by looking at the output power level of a known input signal power. Following that, is the vital noise temperature of the receiver which must obey the protocol requirements. Using the noise figure calculator of the AppCAD from Agilent Technologies, as well as the SystemView simulation, the noise temperature of the receiver is computed. This is followed by the investigation of the dynamic range of the receiver. The receiver dynamic range is set by the minimum and maximum detectable signal power. The investigation of the power levels of these signals is carried out at maximum gain.

The maximum detectable signal power indicates the power level where harmonic distortion begins and inter-modulation products begin to show. This is also confirmed by feeding the receiver with signals larger in amplitude than the maximum detectable signal. This concept is further tested by tracing a small and a large amplitude signal in the receiver chain by means of a graph showing the signal amplitude at consecutive stages of the receiver, taking into account both the minimum and maximum gain of the VGAs.

The chapter ends with two-tone testing, where the power level of the two-tone signal that causes unacceptable inter-modulation products is investigated. Simple CW sinusoidal waveforms are used in the two-tone testing. The other tests that are performed use the simulated DME signals at varying amplitude levels starting from -110 dBm and increasing in 5 dB steps.

It must be stressed that, since the simulated receiver could not be automated, the following tests assume manual mode. Also, only the minimum and maximum gain of the VGAs are

considered in the tests unless otherwise stated.

4.2 System Gain

It is important to know the maximum gain of a receiver because it implicitly informs the receiver designer and or user of the minimum detectable signal. The gain of the simulated L-band RFI measurement receiver is calculated and verified below. Only the minimum and maximum gain of the VGAs are considered in defining the receiver gain. The accumulated gain G_{acc} and the accumulated loss L_{acc} in the receiver front-end from the RF components are calculated below:

$$G_{\text{acc}} \quad G_{\text{LNA}} + G_{\text{WBAMP}} = 36 \mid 14 = 50 \text{ dB} \tag{4.1}$$

$$L_{\text{acc}} \quad L_{\text{switches}} + L_{\text{switchcables}} \mid L_{\text{cables}} \tag{4.2}$$

$$L_{\text{acc}}(\text{dB}) \quad -|(0.4 + 0.3 + 0.3) + (0.25) + (0.2 \mid 0.3 \mid 0.3 \mid 0.3)| = -2.35 \text{ dB} \tag{4.3}$$

where G_{LNA} is the gain of the LNA, G_{WBAMP} is the gain of the wide-band amplifier, and L_{switches}, $L_{\text{switchcables}}$, L_{cables} are losses due to the switches, the switch cables and the cables respectively. The gain of the receiver back-end (Quadrature demodulator electronics) has two values of interest because of the VGAs. Obviously other values are possible but these are not of concern at this stage. Therefore, the AD8347 gain values are:

$$G_{\text{AD8347}}(\text{dB}) \quad G_{\text{RFVGA}} - L_{\text{C}} + G_{\text{IFVGA}} + G_{\text{IF}} \tag{4.4}$$

$$G_{\text{AD8347-max}} = 26 - 6 + 19.5 + 30 \quad 69.5 \text{ dB} \tag{4.5}$$

$$G_{\text{AD8347-min}} = -20 - 6 - 4 + 30 = 0 \text{ dB} \tag{4.6}$$

where G_{RFVGA} is the gain of the RF VGA, G_{IFVGA} is the gain of the IF VGA, G_{IF} is the gain of the baseband amplifier, and L_{c} is the conversion loss of the mixer. Therefore the **maximum and minimum gain of the receiver system** is:

$$G_{\text{sys-max}} \quad G_{\text{acc}} + G_{\text{AD8347-max}} - L_{\text{acc}} - L_{\text{filter}} = 109.45 \text{ dB} \tag{4.7}$$

$$G_{\text{sys-min}} \quad G_{\text{acc}} + G_{\text{AD8347-min}} - L_{\text{acc}} - L_{\text{filter}} = 45.95 \text{ dB} \tag{4.8}$$

where $L_{\text{filter}} = 1.7$ dB is the low-pass filter loss. The maximum gain was verified by setting the VGAs to maximum gain and then feeding the receiver with a signal at -90 dBm. The power spectrum of the output IF signal is shown in Figure 4.1, with the signal power at 18 dBm. This means that the maximum gain of the receiver is 108 dB, a dB less than the computed value.

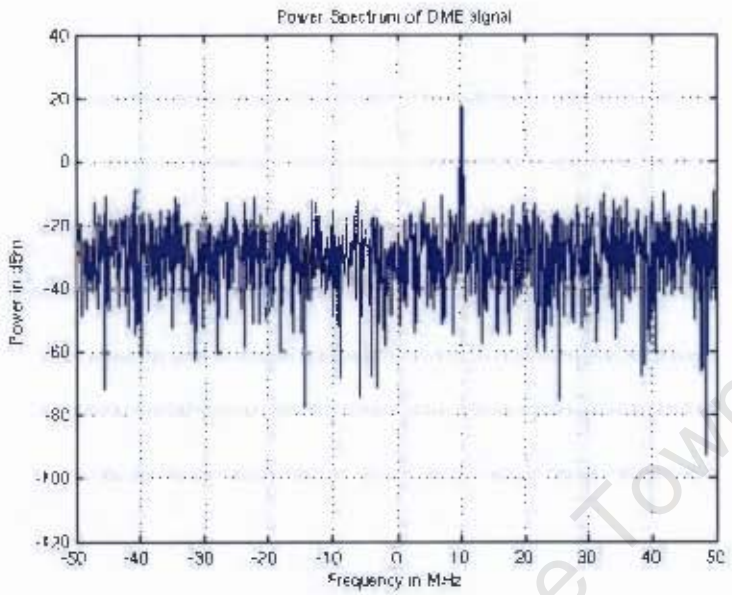

Figure 4.1: Power spectrum of the IF output signal at 10 MHz for an input RF signal at -90 dBm. The IF signal power is at 18 dBm.

4.3 Signal to Noise Ratio and Noise Figure

The noise figure of the simulated receiver is computed using the AppCAD (by Agilent Technologies) noise figure calculator as shown in Figure 4.2. The noise figure calculator is similar to a spreadsheet that replaces the long hand calculation required by equation 4.9:

$$F = F_1 + \frac{F_2 - 1}{G_1} + \frac{F_3 - 1}{G_1 G_2} + \ldots \tag{4.9}$$

where F_n is the noise figure of component number n, where n = 1,2,3,... In SystemView the noise figure calculator values were confirmed as follows. The simulation was ran and the power spectrum plots for the input signal, the in-phase output and the quadrature output were obtained by using the *Power Spectrum dBm into 50 Ohms* calculator. The signal to noise ratio at the input and output of the receiver was obtained by using the **Plot Statistics** button in the Analysis window.

The noise figure of the each chains was obtained by subtracting the signal to noise ratio at the input to the signal to noise ratio at the output of each chain. Thus the noise temperature of the two receiver chains is given by equation 4.10 (([12] page 89-97):

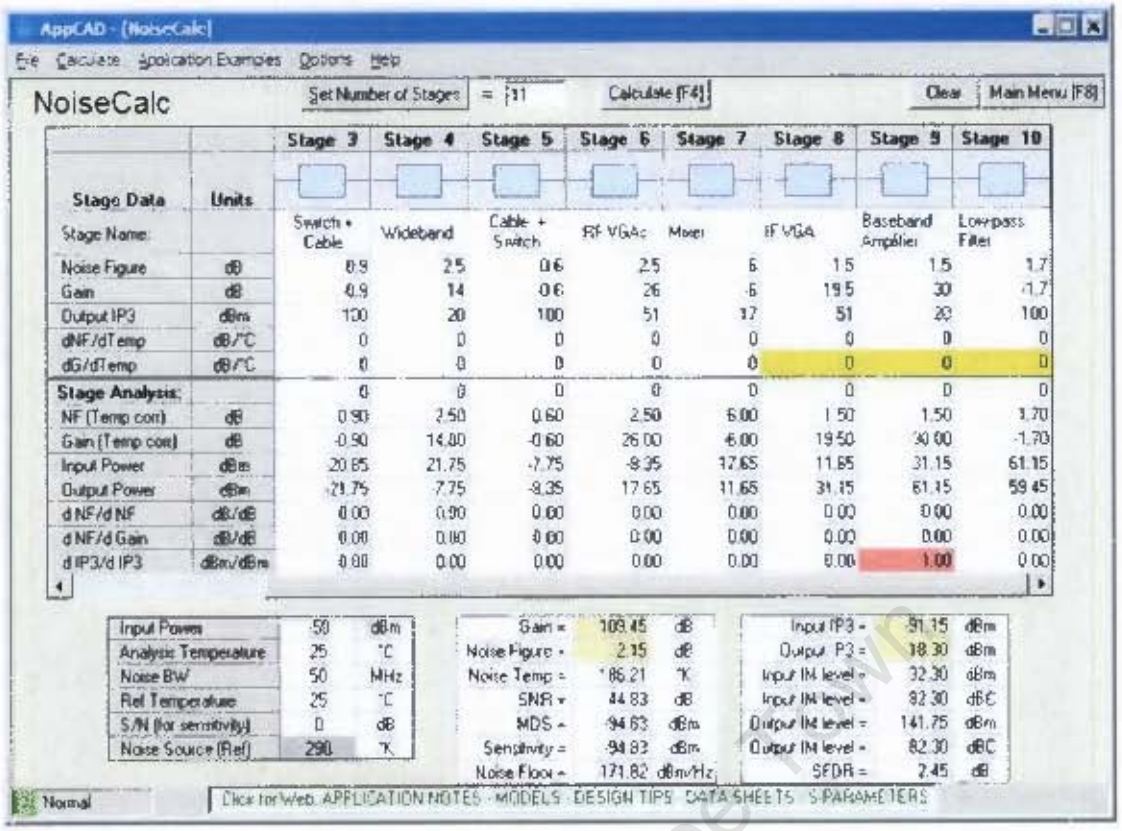

Figure 4.2: Noise Figure Calculator showing the noise temperature of the receiver.

$$T = 290(F - 1) = 186.21 \text{ K} \tag{4.10}$$

where F refers to the linear value of the noise figure, the noise factor. Since the receiver is intended to measure RFI according to the Mode 1 measurements requirements, the calculated receiver temperature meets the protocol specifications for Mode 1 measurements of $T_R < 30\,000$ K. The dynamic range of the receiver is discussed next.

4.4 Dynamic Range

The dynamic range of a receiver is set by the minimum and maximum detectable signal power. For the simulated receiver, the minimum detectable signal power at maximum gain is -100 dBm as shown by the plot of Figure 4.4. When the RF signal power is below -100 dBm, the signal is buried in the noise as shown in Figure 4.3. The maximum detectable signal power is estimated at -59 dBm, meaning that any signal at a power level exceeding this value, will saturate the receiver. Figure 4.5 shows the power spectrum of the IF output for an input at -59 dBm. The undesired spike at -30 MHz confirms the beginning of harmonic distortion already at -59 dBm. The other graphs showing the IF signal power spectrum as the RF signal power is increased are included in Appendix C.

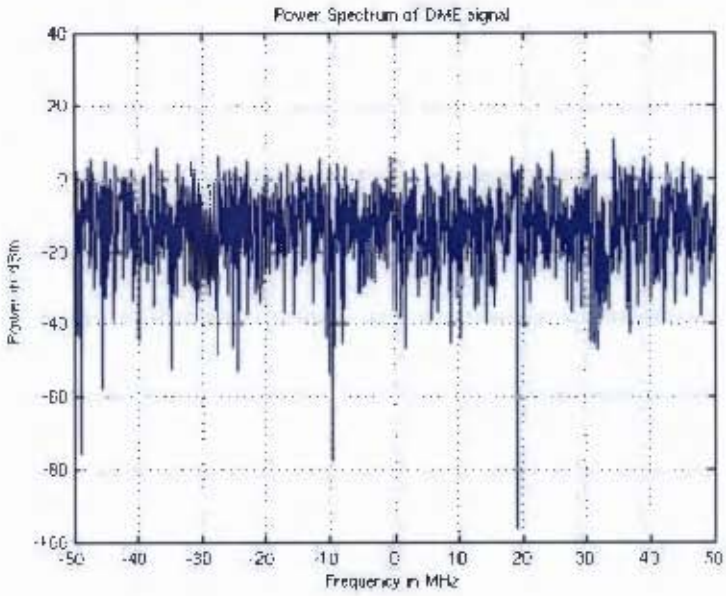

Figure 4.3: Power spectrum of the IF output signal at 10 MHz for an input RF signal at -110 dBm. The figure shows that, power levels below -100 dBm cannot be detected by the receiver.

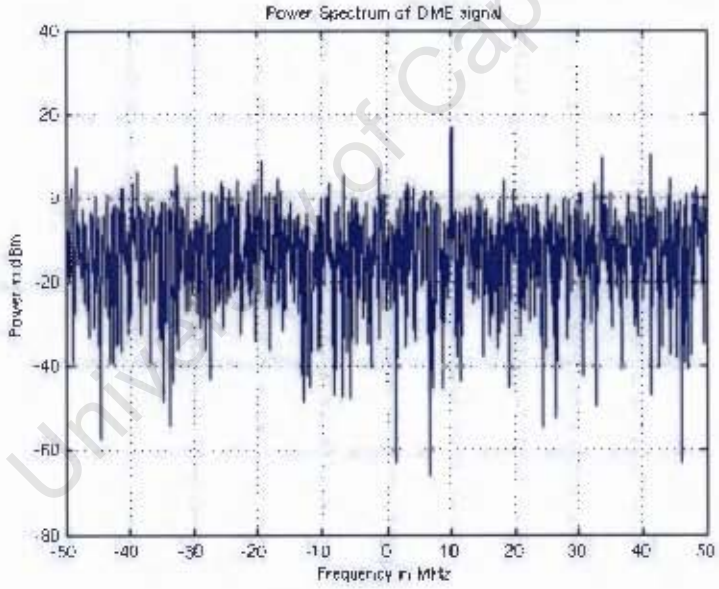

Figure 4.4: Power spectrum of the IF output signal at 10 MHz for an input RF signal at -100 dBm.The figure shows that -100 dBm is the minimum detectable signal.

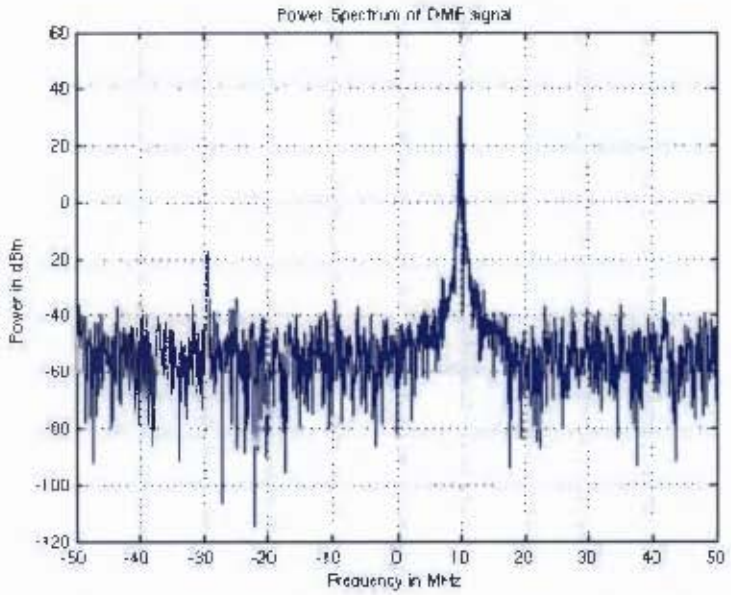

Figure 4.5: Power spectrum of the IF output signal at 10 MHz for an input RF signal at -59 dBm. The figure shows the maximum detectable signal.

Therefore the dynamic range of the simulated receiver at maximum gain is given by ([12], Page 343):

$$DR_r = \frac{\text{Maximum Allowable Signal Power}}{\text{Minimum Detectable Signal Power}} = -59\,\text{dBm} - (-100\text{dBm}) = 41\,\text{dB}$$

4.5 Compression and Third-order Inter-modulation

The power levels that exceed the 1 dB compression point P_1 of an amplifier will cause harmonic distortion and power levels in excess of the third-order intercept point P_3 will cause inter-modulation distortion [12]. Therefore it is important to track the power levels through the stages of the receiver to ensure that P_1 and P_3 are not exceeded. This was conveniently done with a graph as shown in Figure 4.6.

It can be seen that P_1 and P_3 of the amplifiers and mixers are not exceeded as illustrated in Figure 4.6. The P_3 values are not shown in Figure 4.6, because they are well above the P_1. If P_1 cannot be exceeded, P_3 cannot be exceeded as well [12]. Figure 4.6 also depicts the smallest 1 dB compression point.

4.6 Two-tone Testing

A device that adds inter-modulation distortion (IMD) to its output signal will have unwanted frequency components generated at specific frequencies. The third-order products will occur at a frequency of (2*f1 -f2) and (2*f2 - f1), showing up as extra frequency

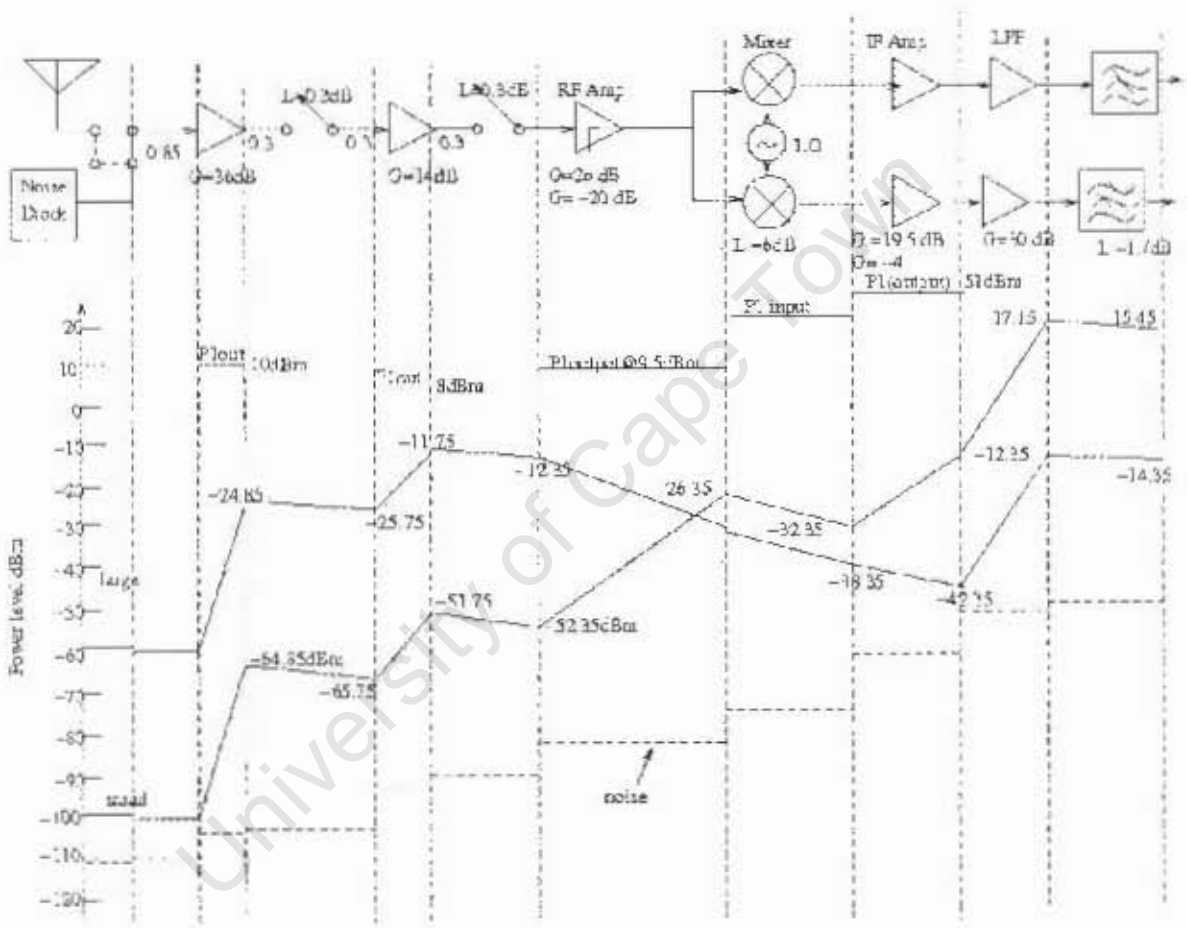

Figure 4.6: Diagram of power and noise levels at consecutive stages of the receiver for a small and large amplitude input signal.

components $\triangle f$ above and below the two input frequencies. Fifth-order IMD will show up as extra frequency components above and below the third-order distortion, exactly $\triangle f$ apart. The other odd-order IMD products will follow suit.

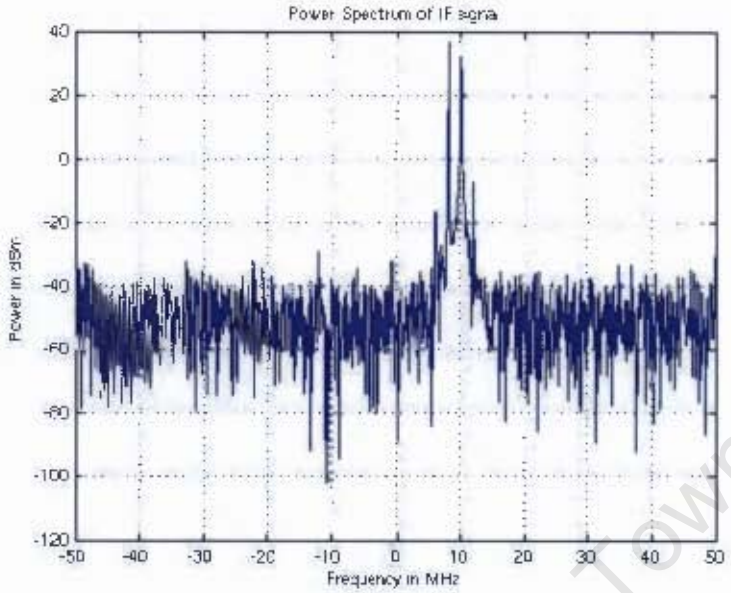

Figure 4.7: Power spectrum of the IF output signals showing the locations and power levels of the 3rd-order products for an input two-tone RF signal at -86 dBm.

The simulated receiver was investigated for this behaviour with an interesting question: at what power level of the input signal will the IMD become severe? The power levels of the input signal was initially set to -100 dBm and increased in 1 dB steps. The RF frequencies are 1029 MHz and 1030 MHz with a local oscillator frequency set at 1020 MHz. The IMD power levels started becoming unacceptable for input power at -85 dBm. Figure 4.7 shows the power spectrum of the IF signal for the two-tone input power of -86 dBm. The two RF frequencies are down-converted into 9 MHz and 10 MHz. The IMD are more than 40 dB below the carrier. For the power level of the two-tone at -85 dBm, the third-order products jump to about 30 dBc as shown in Figure 4.8. However, a two-tone signal with a power level above -85 dBm produces inter-modulation products whose power level is close to the desired IF signals. The plots of the power spectrum for values above -85 dBm are included in Appendix C.

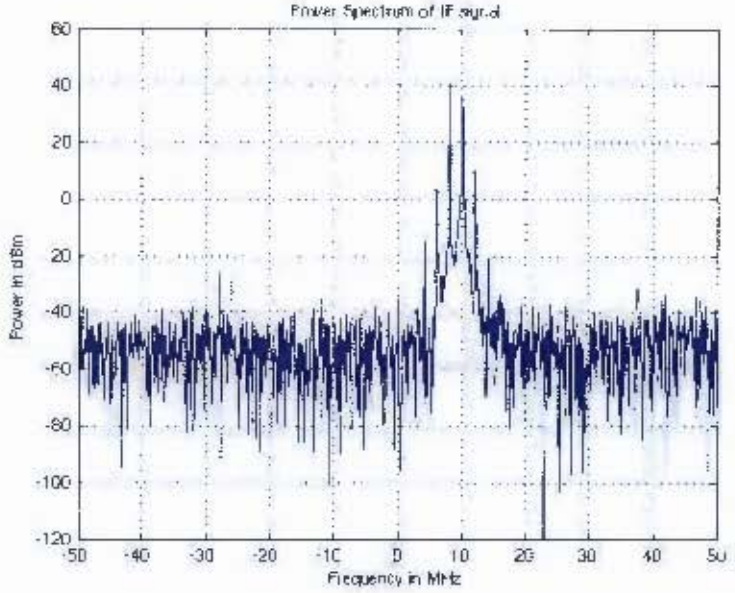

Figure 4.8: Power spectrum of the IF output signals showing the locations and power levels of the 3rd-order products for an input two-tone RF signal at -85 dBm.

4.7 Summary

In summary, the following characteristics of the receiver were investigated. The calculated minimum and maximum gain of the receiver is 45.95 dB and 109.45 dB respectively. The maximum gain was verified in the simulation by setting the VGAs to maximum gain and then feeding the receiver with a signal at -90 dBm. The output was found to be at 18 dBm, meaning that the simulated receiver gain is 108 dB, which is 1.45 dB below the calculated value. Following that was the noise calculations. The noise temperature of the receiver was computed at 7812 K which obeys the protocol requirements for Mode 1 measurements. This is good because the receiver is intended for Mode 1 measurements.

Then the minimum and maximum detectable signal power were measured at -59 dBm and -100 dBm respectively. This means that the dynamic range of the receiver is 41 dB. Subsequently, the small and large amplitude signal were followed throughout the receiver chain to further indicate the minimum and maximum detectable signal power.

Finally, the receiver was tested for two-tone, third-order inter-modulation distortion where it was found that, for a two-tone signal with frequencies 1 MHz apart, the maximum allowable signal power is -85 dBm. If the two-tone signal has a power level above -85 dBm, the 3rd-order products jump to unacceptable levels.

The tests that were done on the practical receiver are documented in the next chapter.

Chapter 5

Practical Tests

This chapter presents the practical tests that were done on the RFI measurement system 4. The purpose of the tests was to ensure that the simulated receiver replicates the practical system and to confirm the simulated receiver predictions. And most importantly, to investigate if DME like signals are correctly measured by the system and do not saturate the receiver.

Because of the difficulty in injecting the signals at the LNA input or via the antenna, it was decided to perform the tests on the demodulator and the digitiser. However, the accumulated gain of the receiver front-end is accounted for in the signal processing. In other words, the RF signal is injected at the RF input of the FPGA where the signal from the antenna mast would normally be connected. The accumulated gain in the receiver front-end is then considered in the signal processing to account for the full receiver chain gain. Otherwise, in practise the receiver back-end (demodulator and digitiser) is sufficient to demonstrate the receiver's capabilities. The terms "receiver" or "system 4 " will be used in this chapter to refer to the receiver back-end being tested.

The receiver is tested using two types of RF signals: the continuous waveform (CW) sinusoidal signals, and the amplitude modulated waveforms with DME signal characteristics. The tests using CW signals are presented first, followed by the amplitude modulated waveforms with DME signal characteristics. The tests using CW signals are done to demonstrate any difference in the way the receiver measures the CW signals to the DME signals.

The receiver has two modes of operation: (i) manual mode and (ii) Automatic Gain Control (AGC) mode. The manual mode is where the gain of the variable gain amplifiers is adjusted manually using a potentiometer. The receiver is tested for performance in both of these modes of operation. The receiver is tested using CW signals in both modes, whereas the DME like signals are only tested in AGC mode. In manual mode, only the minimum and maximum gain is considered as the power level of the RF signal is varied. The tests using the CW sinusoidal signals are presented next.

5.1 Continuous Wave Signals

Two Rohde & Schwarz SML03 signal generators (see Appendix D) are used to produce the RF and LO signals. The power level of the LO oscillator signal is set to -8 dBm as recommended for the AD8347. The RF signal power is increased in steps of 5 dB starting from either -100 dBm or -40 dBm depending on the mode. In manual mode when the gain of the VGAs is set to minimum, the RF signal power starts from -40 dBm. The frequency of the RF and LO signal is 1030 MHz and 1020 MHz respectively. The AD8347 is set to manual mode by adjusting the jumper position on the printed circuit board. The jumper is located next to the potentiometer as shown in Figure 5.1.

Figure 5.1: Printed circuit board showing the demodulating electronics. The jumper is to the right of the light blue potentiometer.

Figure 5.1 shows the jumper position under Automatic Gain Control mode. Moving the jumper position to the right will set the demodulator to manual mode. The minimum gain of the VGAs is obtained by turning the potentiometer fully anti-clockwise, and vice-versa for the maximum gain. The manual mode tests are presented next.

5.1.1 Manual Mode

Under manual mode of the demodulator, only the minimum and maximum gain conditions are investigated. This is because any gain value in between the minimum and maximum gain is what the VGAs usually take under AGC mode. The receiver is tested for the

following characteristics: the minimum and maximum detectable signal, the dynamic range, and saturation or compression. The noise figure and the SNR are dealt with in the simulation as it is difficult to calculate or estimate the SNR at the input in the practical setup. The inter-modulation distortion is also considered in the simulated receiver. If the simulation replicates the receiver, the tests done in the simulation can be considered accurate and a very close estimation of how the real receiver would behave.

In all of the following plots the LO frequency, 1020 MHz, represents 0 MHz in the figure. In other words, the zero is at 1020 MHz such that the IF is located 10 MHz away from the LO at 1010 MHz. The red plot in all the graphs shown in this chapter is the minimum trace that is set to catch the dying transients.

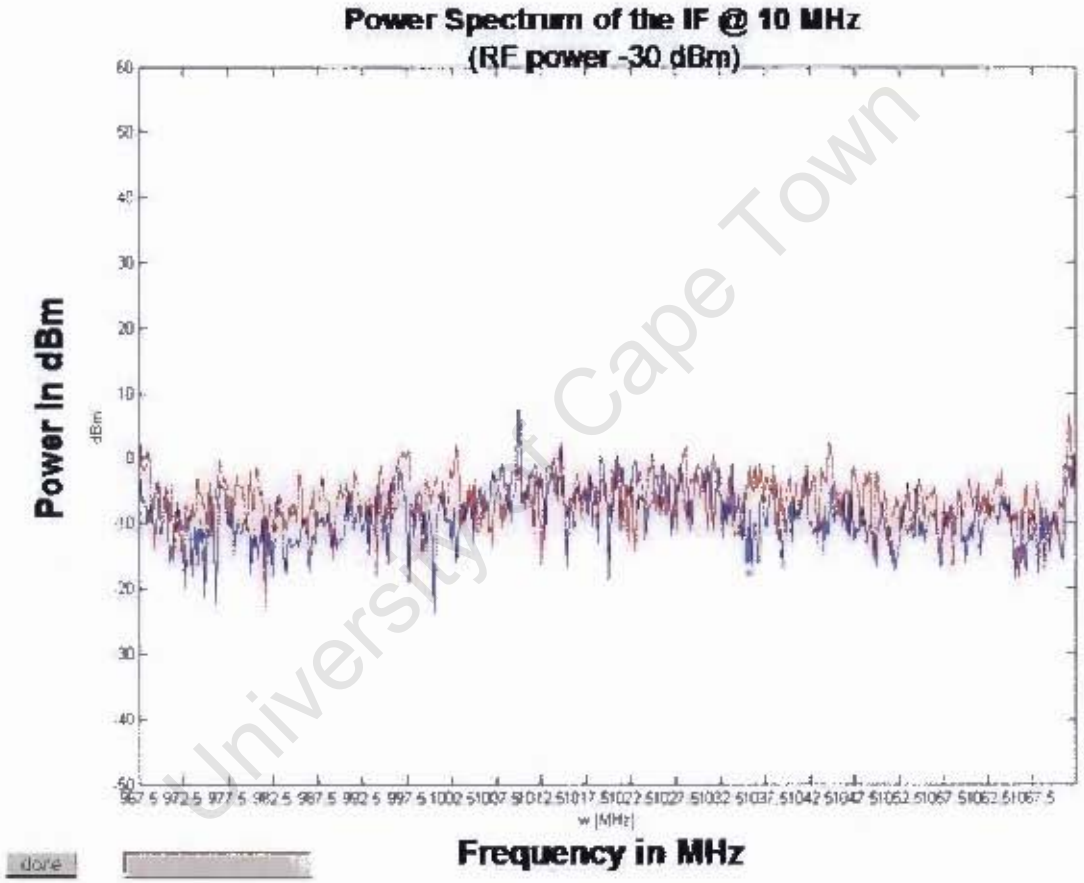

Figure 5.2: Power spectrum of the output IF signal at 10 MHz (or 1010 MHz in the figure) for an RF input signal power of -30 dBm.

Minimum Gain

The VGAs were set for minimum gain using the potentiometer as described above, and the RF signal power was initially set to -40 dBm then the power spectrum of the output IF signal was observed. The IF signal was buried in the noise and could not be detected. The power of the RF signal was then increased in steps of 5 dB and the minimum detectable signal power was at -30 dBm. The power spectrum of the IF output signal for

the minimum detectable signal power, -30 dBm, at minimum gain is shown in Figure 5.2 above.

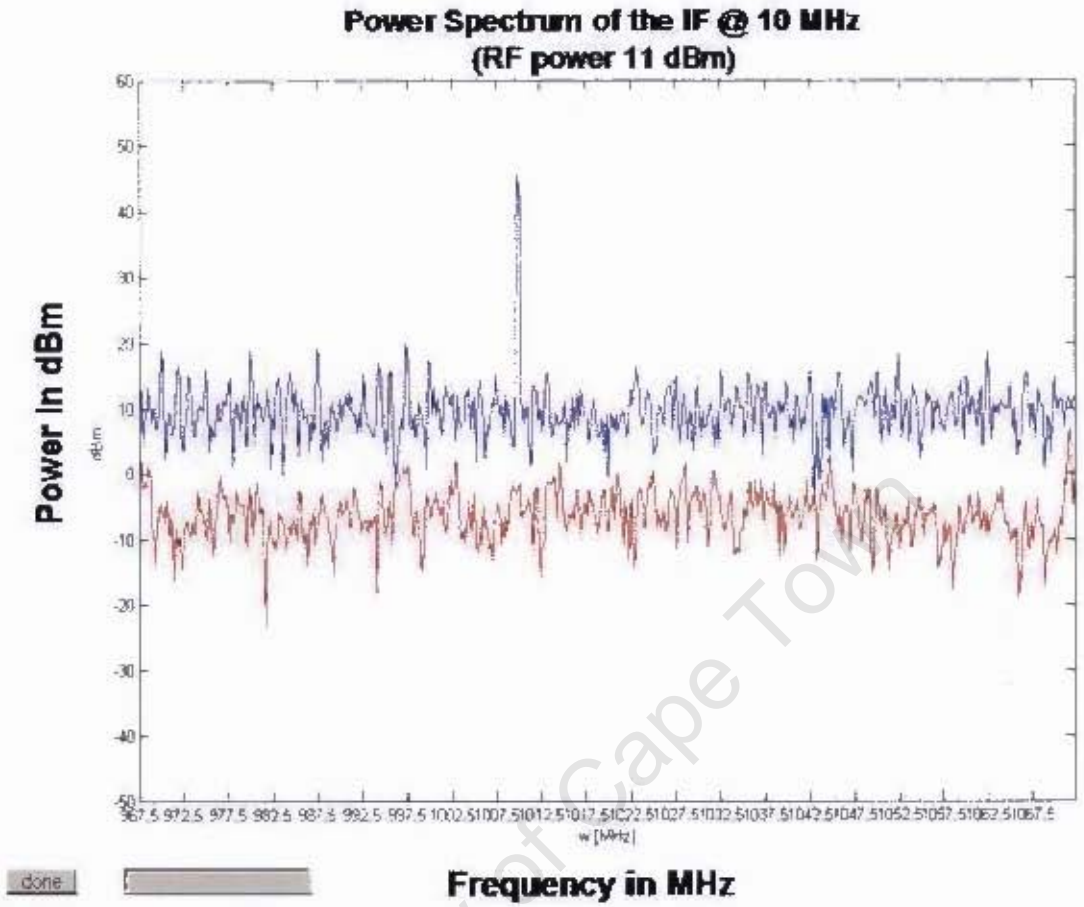

Figure 5.3: Power spectrum of the output IF signal at 10 MHz (or 1010 MHz in the figure) for an RF input signal power of 11 dBm.

The power level of the RF signal was increased again until the receiver started showing saturation and producing inter-modulation products. The power spectrum of the IF output signal for the maximum detectable signal power is shown in Figure 5.3 above. It is important to notice that the average noise level has jumped up to about 10 dBm from about -10 dBm at the minimum detectable signal power. Any RF signal above 11 dBm causes inter-modulation distortion. The red plot in figure above tracks the minimum traces in order to catch the transients. The graphs showing the IF power spectrum as the RF signal power increases are included in Appendix D. The findings of the receiver tests performed using the minimum gain under manual mode are summarised in Table 5.1.

Table 5.1: **Receiver tests findings using minimum gain under manual mode.**

Parameter	Value
Min. Detectable Signal	-30 dBm
Max. Detectable Signal	11 dBm
Dynamic Range	41 dB
Gain Receiver	38 dB

In terms of the main objective that the receiver was built for, the findings in the table above can be interpreted as follows. The receiver is an L-band receiver designed to measure RFI in this band, including DME. If the demodulator, under manual mode, minimum gain operation, has a minimum detectable signal of -30 dBm. Then the smallest receivable DME signal power calculated in Chapter 3 cannot be detected by the receiver. Therefore the DME signals will *only* be detected when the aircraft is at the following slant range distance from the measurement system (or closer):

$$P_{r-}\,[\text{dBm}] = P_t\,[\text{dBm}] + G_t\,[\text{dB}] + G_r\,[\text{dB}] - 10\log(\frac{4\pi R}{\lambda})^2 \tag{5.1}$$

$$\text{-30 dBm} = 49.42\ \text{dBm} + 0\ \text{dB} + 6.5\ \text{dB} - 10\log(\tfrac{4\pi R}{\lambda})^2$$

$$R = 410\ \text{m}$$

Since it is very unlikely to have transmitting aircrafts flying 410 meters to the receiver. This means that this kind of a receiver setup is not desirable. Therefore, manual mode of the AD8347 and minimum gain of the VGAs is not an option for detecting RFI in the L-band and particularly DME interference.

Maximum Gain

The same tests that were done using the minimum gain of the VGAs were repeated for the maximum gain. The dynamic range was expected to remain the same as in the minimum gain, but of interest this time was the minimum and maximum detectable signal power. The power spectrum of the IF output signal for the minimum detectable signal power at maximum gain is shown in Figure 5.4. And the power spectrum of the IF output signal for the maximum detectable signal power is shown in Figure 5.5.

It essential to note that the practical system has a purpose-written software that does FFT in Matlab and plot not only the power level(s) of the instantaneous signal(s), but also tracks the minimum traces in order to catch transients at lower power levels. The red plot in all the graphs shown in this chapter is the minimum trace that is set to catch the dying transients.

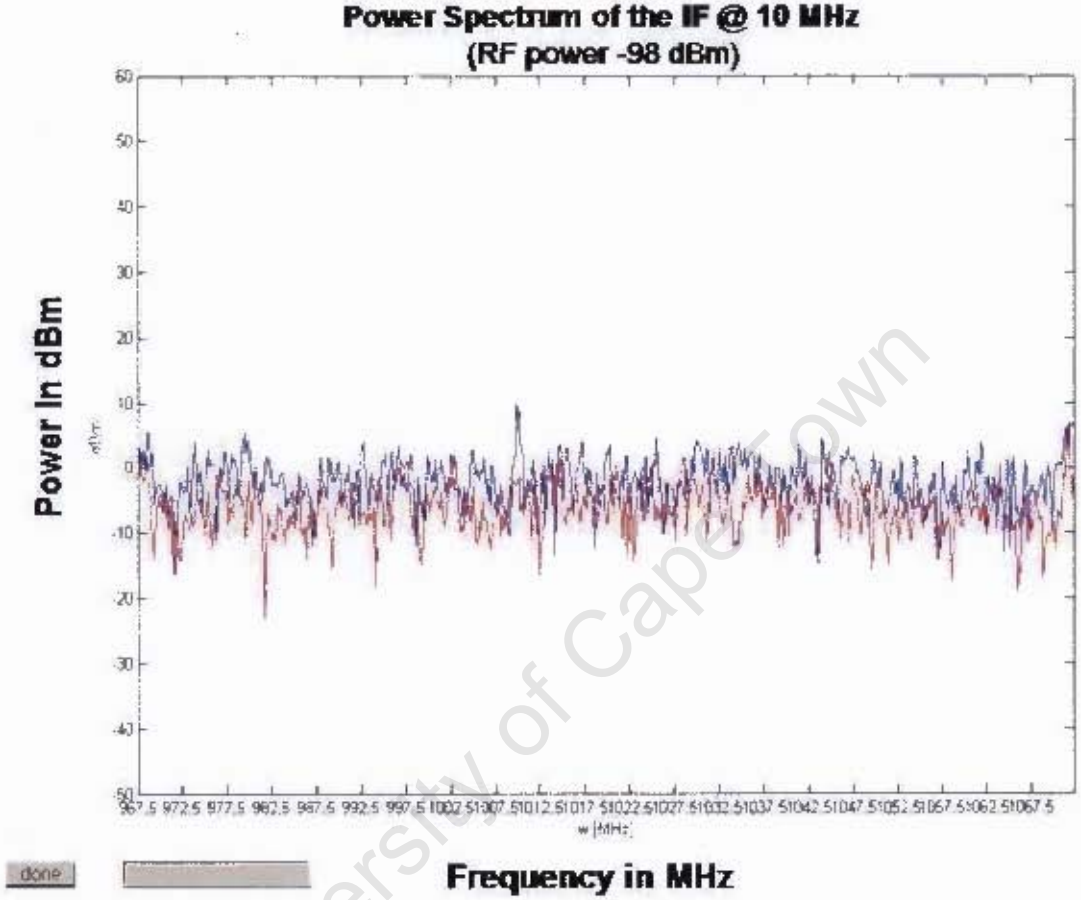

Figure 5.4: Power spectrum of the output IF signal at 10 MHz for an RF input signal power of -98 dBm. This figure shows the minimum detectable signal power at maximum gain.

The dynamic range is calculated at 39 dB which is at 2 dB below that for the minimum gain. The gain of the receiver at maximum gain is 108 dB, which is more than twice the receiver gain at minimum gain. It is interesting to note that this gain value corresponds with the value obtained in the simulation. Table 5.2 summarises the findings.

Table 5.2: **Receiver tests findings using maximum gain under manual mode.**

Parameter	Value
Min. Detectable Signal	-98 dBm
Max. Detectable Signal	-59 dBm
Dynamic Range	39 dB
Gain Receiver	108 dB

This receiver setup will be able to detect and measure RFI caused by DME signals whose

source is an aircraft 250 km away from the receiving system and further away. However, a maximum detectable signal of -59 dBm means that any DME transmitter closer than 11.5 km will saturate the receiver. The closest known DME ground station is in Sutherland which is more than 150 km from the core site. It is therefore very unlikely to have DME transmitters as close as 11.5 km from the core. Therefore, the receiver can be operated in manual mode using maximum gain provided the interference source is 11.5 km away or more. It is worth noting that these values correspond to the values found in the simulation tests.

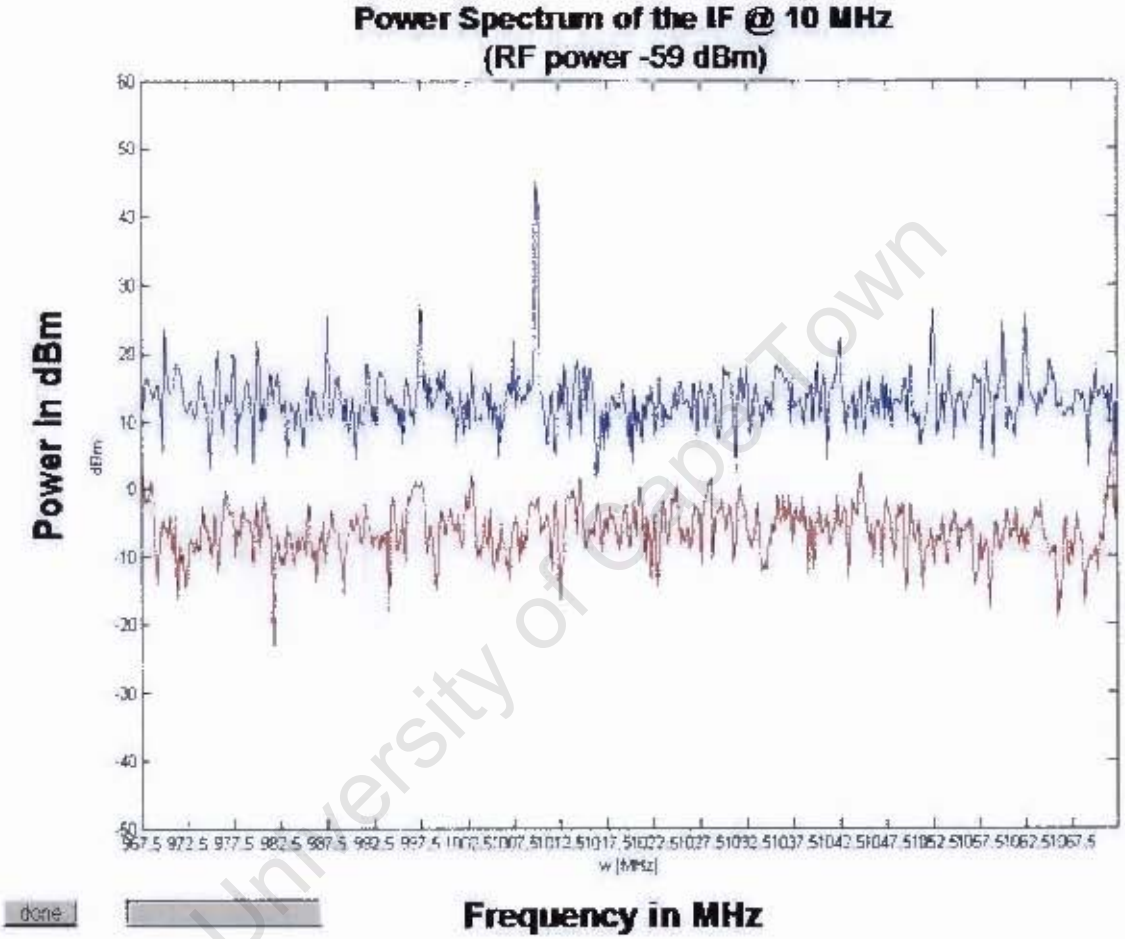

Figure 5.5: Power spectrum of the output IF signal at 10 MHz for an RF input signal power of -59 dBm. This figure shows the maximum detectable signal power at maximum gain.

5.1.2 Automatic Gain Mode

Using a CW signal, the receiver was set to AGC mode. The RF signal power was varied starting from -110 dBm where the output signal was buried in the noise. At an RF power level of -96 dBm the output IF signal could be observed. The -96 dBm power is therefore the minimum detectable signal power under AGC mode, Figure 5.6. In steps of 5 dB, the gain of the signal was increased and the output IF plots were saved into a disk and are included in Appendix D. Figure 5.7 shows the maximum detectable signal power at 10 dBm. This means that the receiver's dynamic range is 106 dB which is a very good

dynamic range. The difference between the output and input signal power gives the gain which varies with the amplitude of the input signal. The gain varies with the amplitude of the input signal between 34 and 106 dB.

Although the receiver gain and dynamic range are relatively higher in AGC mode. The changing gain is not appropriate for RFI measurements. This is because of the following reason. The AGC compensation loop has a time constant set by a 0.1μF capacitor to adjust the power output to the desired level. The real world interference on the other hand, will be entering the receiver at random power levels, impulsively and very rapidly. This means that the compensation loop will be constantly striving to adjust the AGC of the receiver, as a result the power level measured at the output will not necessarily be the true power of the received signal(s). Therefore, the raw data from the digitiser cannot be calibrated since the gain of the AGC is unknown. In other words, power level measurements cannot be made since an unknown AGC is switched on. **It is therefore only appropriate to perform RFI measurements under manual mode, moderate or maximum gain.** In this way the receiver can be calibrated before measurements, and the data obtained from the digitiser can then be calibrated using a known receiver gain.

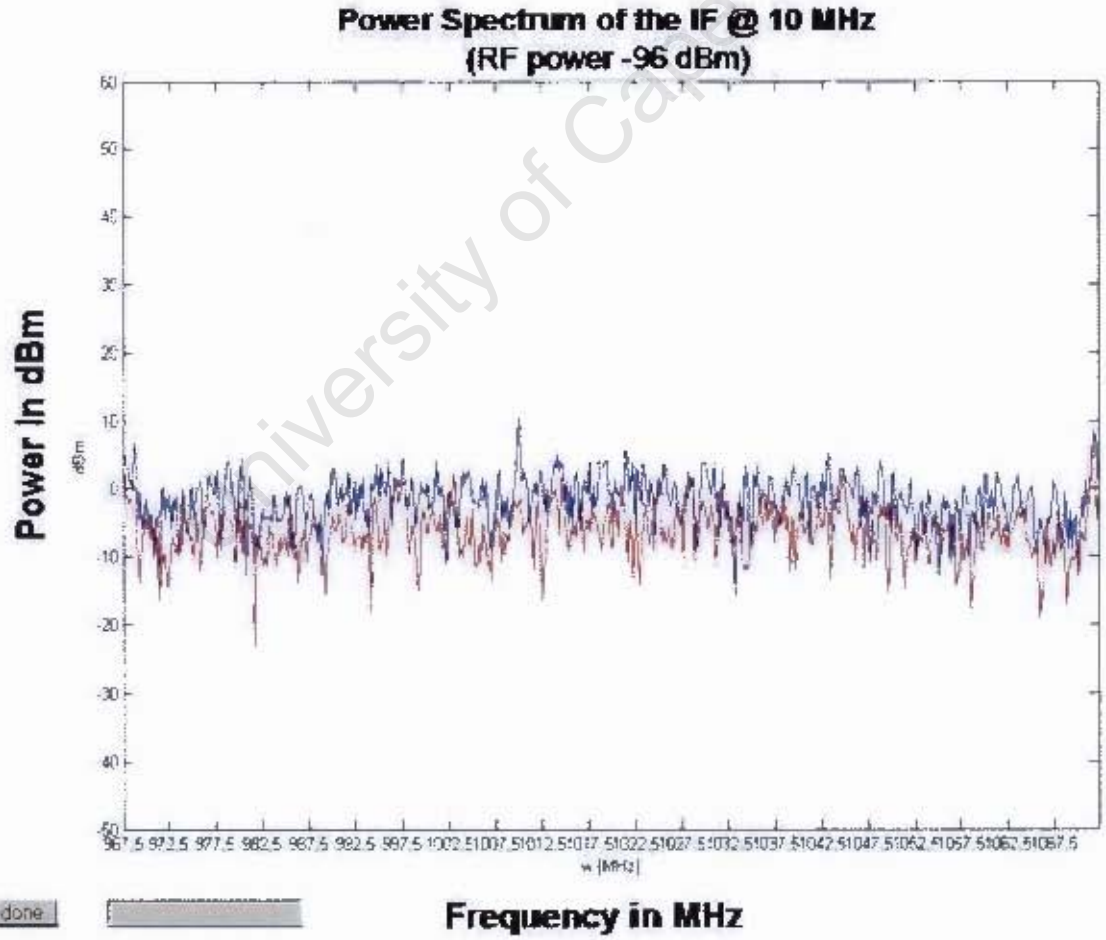

Figure 5.6: Power spectrum of the IF signal at 10 MHz for an RF input signal power of -96 dBm. This figure serves to show the minimum detectable signal under AGC mode.

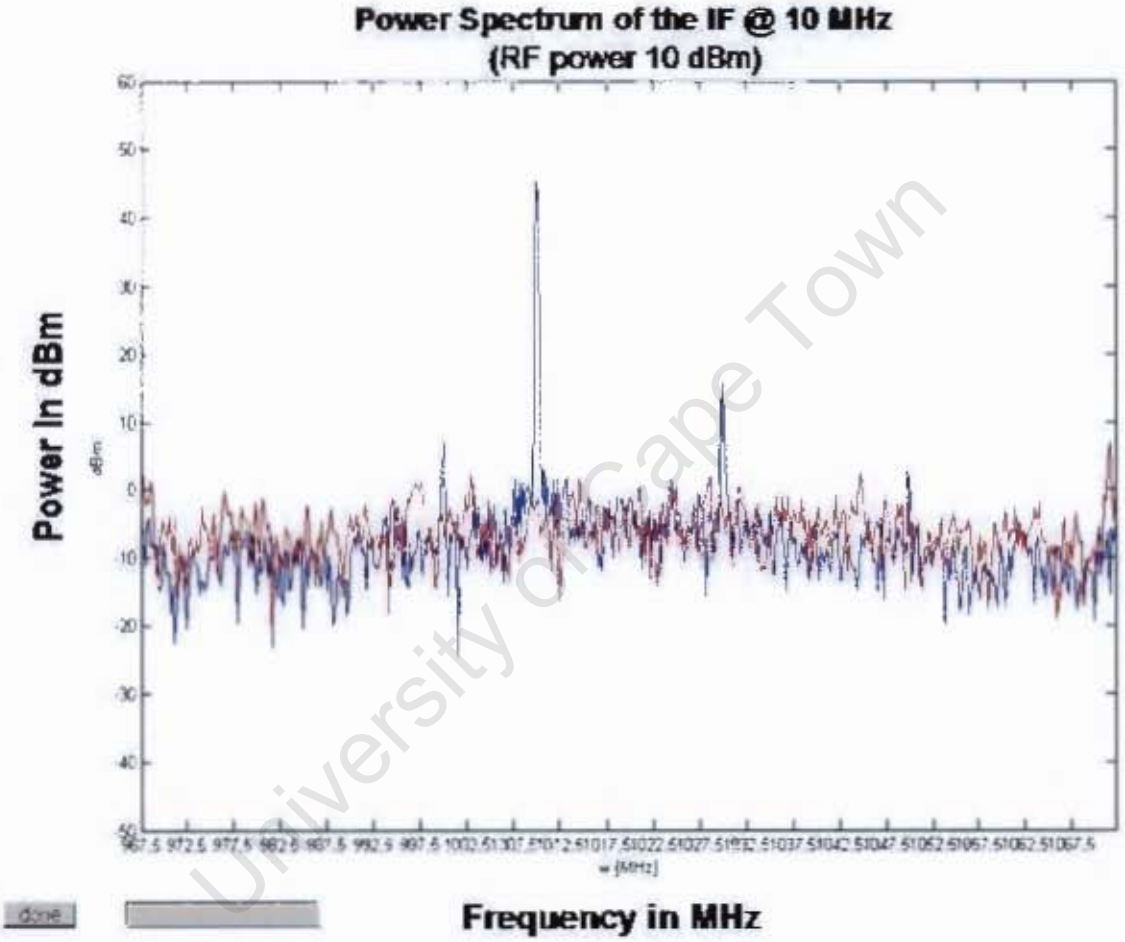

Figure 5.7: Power spectrum of the output IF signal at 10 MHz for an RF input signal power of 10 dBm. This figure serves to show the maximum detectable signal under AGC mode.

5.2 Amplitude Modulated Signals

A signal generator was used to produce amplitude modulated signals. The shape of the modulated waveforms was square, with a pulse width of 3.5 μs and a pulse period 12 μs. The carrier frequency was set to 1030 MHz and the local oscillator frequency was 1020 MHz. By default the minimum signal power of the generator used for these measurements is -5 dBm. This means the minimum detectable signal power for the amplitude modulated signals with DME characteristics could not be tested. The only obvious choice would be to use an attenuator to drop the power level coming out of the signal generator. The availability of such an attenuator was the only problem in pursuing this idea. The receiver was therefore tested (without the attenuator) using an RF signal with a power level of -5 dBm. The power level was increased in steps of 1 dB.

The red plot tracks the minimum traces in order to catch the transients. The plot that tracks maximum traces has been removed in all the graphs. This is because maximum trace plot covers the plot of the signal of interest.

5.2.1 Maximum Detectable Signal

Using the amplitude modulated, DME-like signals, the maximum detectable signal in AGC mode was investigated. Figure 5.8 shows the output IF when the input signal is at the maximum detectable signal power.

The results obtained using the simulator and the practical receiver are discussed next.

5.3 Simulation vs Practical System

The simulation is not automated like the real system but under manual mode, maximum gain, the simulation is a replica of the real system. This is because the gain, the dynamic range, and the minimum and maximum detectable signal power values of the simulation correspond to within 1 dB with the practical system values. Therefore conclusions on the behaviour of the real system can be drawn based on the simulation behaviour. This means that, DME signals of various amplitudes and frequencies can be simply investigated in the simulation, and the results can be assumed in the real system provided the same mode is assumed.

In manual mode, maximum gain, the results in Table 5.3 were obtained for the simulation and the practical receiver. The maximum detectable signal is the signal, which corresponds to a distance of 11.5 km in slant range. In other words, the RFI measurement system will be saturated by interference sources closer than 11.5 km. It is very unlikely to have L-band interferences closer than 11.5 km at the core site since the closest DME ground stations are at Sutherland which is more than 150 km from the core site. However, should the interference sources be closer than 11.5 km, then the gain of the VGAs can

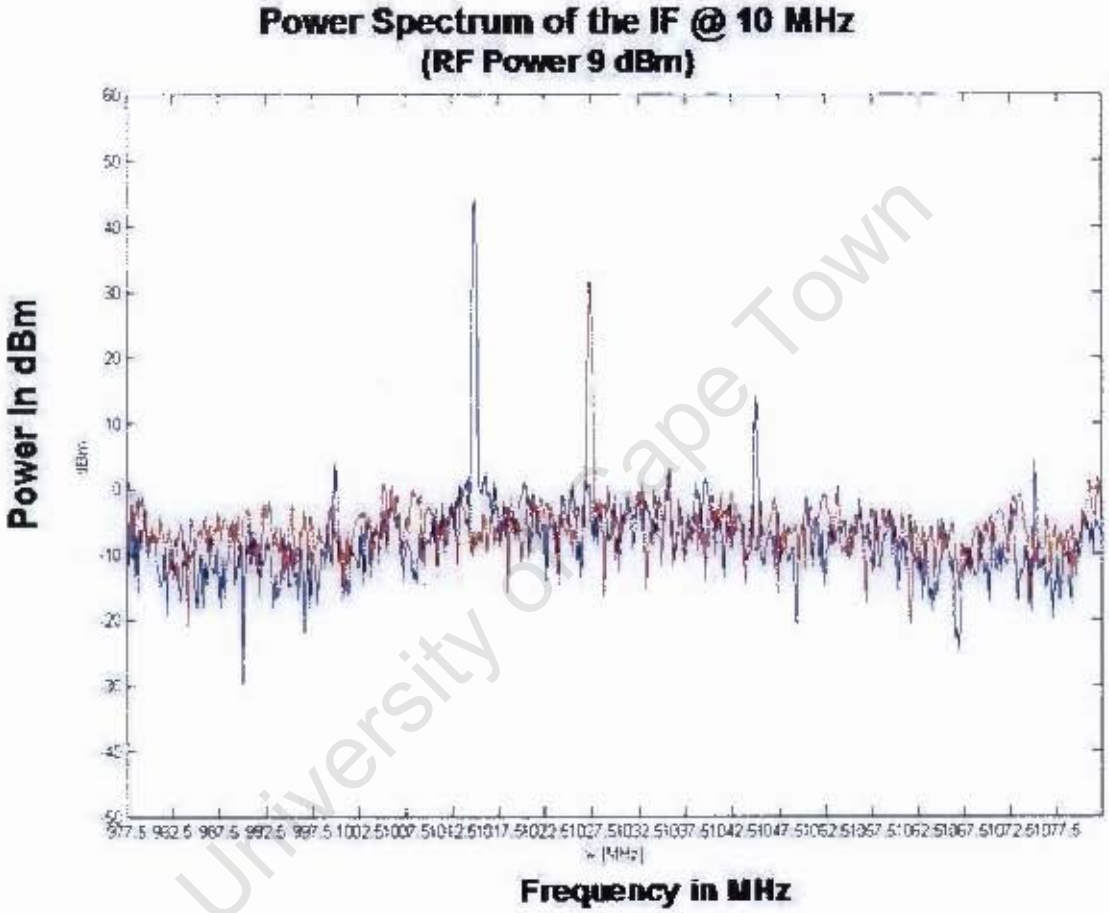

Figure 5.8: Power spectrum of the output baseband signal at 10 MHz for an RF input signal power of 9 dBm. The figure shows the output of the maximum detectable signal power.

be manually adjusted to a moderate value and the system can then be calibrated based on that gain value.

It can therefore be concluded that manual mode is appropriate for RFI measurements since the gain of the receiver remains unchanged. This forms a good basis for calibrating the RFI measurement set and producing the required graphs in the RFI protocol. Table 5.3 clearly shows that the simulation and the practical system are exact replicas of each other, at least in manual mode.

Table 5.3: **Simulation versus the Practical System in manual mode maximum gain.**

Parameter	Simulation	Practical
$G_{\text{sys-max}}$	108	108
Dynamic Range	41	39
Max. Detectable Signal	-59 dBm	-59 dBm
Min. Detectable Signal	-100 dBm	-98 dBm

Table 5.4: **AGC mode results using CW signals.**

Parameter	Value
Max. Detectable Signal	9 dBm
Min. Detectable Signal	-96 dBm
Dynamic Range	105 dB
Gain	34 to 106 dB

In AGC mode, using CW signals the results in Table 5.4 were obtained. Even though the minimum detectable signal power could not be investigated using DME-like signals in the practical system. The value obtained using CW signals can be used as a guideline. In AGC mode, CW signals tests, the minimum detectable signal is -96 dBm. This value is most likely to hold for the DME like signals or vary by one dB. Therefore, the receiver will still have about 105 dB of dynamic range when measuring DME like signals. The dynamic range is best under AGC mode and the maximum detectable signal power is higher. Up to about 8 mW could be detected before inter-modulation products are visible and unacceptable. But the changing gain is undesired in RFI measurements based on the protocol specifications, and thus AGC mode is undesirable in our intended application. The next chapter draws conclusions on the work that was done.

Chapter 6

Conclusions and Recommendations

This chapter documents the conclusions made from the study and presents the recommendations for better receiver performance, and particularly how to measure burst mode RFI in the L-band using this receiver.

6.1 Conclusions

The conclusions of this thesis project are as follows:

- The RFI measurement system 4, can and will measure DME RFI without suffering from compression and inter-modulation distortion.
- Manual mode and maximum gain is the preferred choice, but care must be taken for interference sources closer than 11.5 km as they will saturate the receiver. In this case, moderate gain will have to be used and the data calibrated accordingly.
- The measurement of RFI in AGC mode is forbidden since the gain of the AGC is unknown and thus calibration is impossible.

To summarise the thesis objectives and how they have been met, the following can be said:

- The SKA Memo 37 was reviewed and its requirements were understood and summarised in Chapter 2.
- The L-band RFI measurement receiver was simulated in SystemView and the simulation used the real receiver as the simulation gel.
- The receiver was found to conform to the requirements in Table 1 of the SKA Memo 37.
- The DME signals characteristics were researched and simulated in SystemView. These signals were used as the input to the receiver.

- The receiver was then investigated for minimum and maximum detectable signals. Saturation was also investigated where it was found that the receiver can withstand power levels up to 10 dBm in AGC mode and sources as close as 11.5 km in manual mode.
- As a final conclusion, it was found that the receiver can measure impulsive RFI in the L-band.
- The appropriate choice for the measurement of RFI was found to be manual mode.

6.2 Recommendations

The following recommendations are drawn from the study:

1. It is recommended that the receiver's demodulator be operated in manual mode when RFI measurements are to be made.
2. If the receiver is to be operated in manual mode, the minimum gain of the VGAs must never be utilised.
3. The mismatch between the filters can be improved, this is suspected to reduce false alarm in the detection of very low power transients.

6.3 Closing Remarks

The Square Kilometer Array must be located in a remote area. This requires a thorough investigation of Radio Frequency Interference at the site of choice. The systems used to measure the RFI must conform to the RFI Protocol compiled by the Working Group on RFI. The use of a spectrum analyzer to measure in the L-band does not agree with the protocol requirements for Mode 1 measurements. As a result, an FFT spectrometer was proposed and built. This thesis was investigating the capability of such an instrument to measure RFI as required by the protocol. The proposed system was found to measure RFI as expected. It is strongly recommended that the receiver be operated in manual mode, maximum gain during RFI measurements.

Bibliography

[1] SKA South Africa website, Brochure, www.ska.ac.za/docs.html

[2] International SKA Website, www.skatelescope.org

[3] SA SKA RFI team, "Analysis of the Radio Frequency Environment", March 2006.

[4] SKA South Africa website, www.ska.ac.za

[5] SKA South Africa, ANNEXURE 3, RFI Measurements, Preliminary RFI Reports at the Kalahari site, November 2003, www.ska.ac.za/docs.html.

[6] SA SKA Team, South African SKA Project, "Final Proposal for RFI Equipment",2004.

[7] **Working Group on RFI Measurements**, R. Ambrosini, R. Beresford, A.J. Boonstra, S. Ellingson, K. Tapping, RFI Measurement Protocol for Candidates SKA Sites. SKA Site Evaluation and Selection Committee, May 2003.

[8] S. W. Ellingson and G. A. Hampson, Mitigation of Radar Interference in L-Band Radio Astronomy, The Ohio State University, ElectroScience Laboratory, February 2003.

[9] R. P. Millenaar, A.J. Boonstra, SKA Spectrum Monitoring Plan for Candidates Sites, January 2004.

[9] J. R. Fisher, Signal Analysis and Blanking Experiments on DME Interference, National Radio Astronomy Observatory, Green Bank, West Virginia, ELECTRONICS DIVISION INTERNAL REPORT NO. 313, April 2004.

[11] Republic of South Africa SKA Bid, Proposal to site the Square Kilometre Array, March 2005

[12] David M. Pozar, Microwave and RF Design of Wireless Systems, John Wiley & Sons, New York, 2001

[13] National Radio Astronomy Observatory, www.nrao.edu/whatisra/rfi.shtml

[14] Analog Devices, AD8347 Data Sheet, www.analogdevices.com

[15] MiniCircuits, www.minicircuits.com

[16] Miteq, www.miteq.com

[17] S. W. Ellingson, G.A. Hampson, Mitigation of Radar Interference in L-band Radio Astronomy, The Ohio State University, Astrophysical Journal Supplement Series, 147:167-176, July 2003.

[18] F. H. Briggs, J. F. Bell, M. J. Removing Radio Interference from Contaminated Astronomical Spectra using and independent reference signal and closure relations, Astronomical Journal, 120:3351-3361, December 2000.

[19] Qing Zhang, Yibin Zheng, Stephen G. Wilson, and J. Richard Fisher and Richard Bradley, Combating Pulsed Radar Interference in Radio Astronomy, Astronomical Journal, 126:1588-1594, September 2003.

[20] J. R. Fisher, Q. Zhang, Y. Zheng and S. G. Wilson and R.F. Bradely, Mitigation of Pulsed Interference to Redshifted H I and OH Observations Between 960 and 1215 MEGAHERTZ, Astronomical Journal, 129:2940-2949, June 2005.

[21] Qing Zhang, Yibin Zheng, Stephen G. Wilson, and J. Richard Fisher and Richard Bradley, Excision of Distance Measuring Equipment Interference From Radio Astronomy Signals, Astronomical Journal, 129:2933-2939, June 2005.

Appendix A

AD8347 Demodulator Data sheet

This appendix documents the specifications of the AD8347 quadrature demodulator as found in the data sheet that was obtained from the manufacturer. The data sheet can be found from the Analog Devices website but is included here for completeness.

0.8 GHz to 2.7 GHz Direct Conversion Quadrature Demodulator

AD8347

FEATURES

Integrated RF and baseband AGC amplifiers
Quadrature phase accuracy 1° typ
I/Q amplitude balance 0.3 dB typ
Third-order intercept (IIP3) +11.5 dBm @ min gain
Noise figure 11 dB @ max gain
AGC range 69.5 dB
Baseband level control circuit
Low LO drive −8 dBm
ADC-compatible I/Q outputs
Single supply 2.7 V to 5.5 V
Power-down mode
28-lead TSSOP package

APPLICATIONS

Cellular base stations
Radio links
Wireless local loop
IF broadband demodulators
RF instrumentation
Satellite modems

FUNCTIONAL BLOCK DIAGRAM

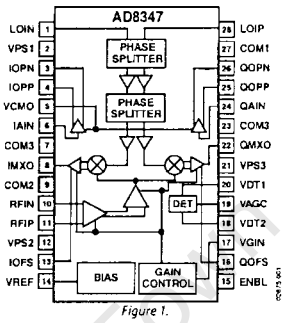

Figure 1.

GENERAL DESCRIPTION

The AD8347[1] is a broadband direct quadrature demodulator with RF and baseband automatic gain control (AGC) amplifiers. It is suitable for use in many communications receivers, performing quadrature demodulation directly to baseband frequencies. The input frequency range is 800 MHz to 2.7 GHz. The outputs can be connected directly to popular A-to-D converters such as the AD9201 and AD9283.

The RF input signal goes through two stages of variable gain amplifiers prior to two Gilbert-cell mixers. The LO quadrature phase splitter employs polyphase filters to achieve high quadrature accuracy and amplitude balance over the entire operating frequency range. Separate I and Q channel variable gain amplifiers follow the baseband outputs of the mixers. The RF and baseband amplifiers together provide 69.5 dB of gain control. A precision control circuit sets the linear-in-dB RF gain response to the gain control voltage.

Baseband level detectors are included for use in an AGC loop to maintain the output level. The demodulator dc offsets are minimized by an internal loop, whose time constant is controlled by external capacitor values. The offset control can also be overridden by forcing an external voltage at the offset nulling pins.

The baseband variable gain amplifier outputs are brought off-chip for filtering before final amplification. By inserting a channel selection filter before each output amplifier, high level out-of-channel interferers are eliminated. Additional internal circuitry also allows the user to set the dc common-mode level at the baseband outputs.

[1] U.S. patents issued and pending.

One Technology Way, P.O. Box 9106, Norwood, MA 02062-9106, U.S.A.
Tel: 781.329.4700 www.analog.com
Fax: 781.461.3113

SPECIFICATIONS

V_S = 5 V; T_A = 25°C; F_{LO} = 1.9 GHz; V_{VCMO} = 1 V; F_{RF} = 1.905 GHz; P_{LO} = −8 dBm, R_{LOAD} = 10 kΩ, dBm with respect to 50 Ω, unless otherwise noted.

Table 1.

Parameter	Conditions	Min	Typ	Max	Unit
OPERATING CONDITIONS					
LO/RF Frequency Range		0.8		2.7	GHz
LO Input Level		−10		0	dBm
VGIN Input Level		0.2		1.2	V
V_{SUPPLY} (V_S)		2.7		5.5	V
Temperature Range		−40		+85	°C
RF AMPLIFIER/DEMODULATOR	From RFIP/RFIN to IMXO and QMXO (IMXO/QMXO load > 1 kΩ)				
AGC Gain Range			69.5		dB
Conversion Gain (Max)	V_{VGIN} = 0.2 V (max gain)		39.5		dB
Conversion Gain (Min)	V_{VGIN} = 1.2 V (min gain)		−30		dB
Gain Linearity	V_{VGIN} = 0.3 V to 1 V		±2		dB
Gain Flatness	F_{LO} = 0.8 GHz to 2.7 GHz, F_{BW} = 1 MHz		±0.7		dB p-p
Input P1 dB	V_{VGIN} = 0.2 V		−30		dBm
	V_{VGIN} = 1.2 V		−2		dBm
Third-Order Input Intercept (IIP3)	F_{RF1} = 1.905 GHz, F_{RF2} = 1.906 GHz, −10 dBm each tone, (min gain)		+11.5		dBm
Second-Order Input Intercept (IIP2)	F_{RF1} = 1.905 GHz, F_{RF2} = 1.906 GHz, −10 dBm each tone, (min gain)		+25.5		dBm
LO Leakage (RF)	At RFIP		−60		dBm
LO Leakage (MXO)	At IMXO/QMXO		−42		dBm
Demodulation Bandwidth	−3 dB		+90		MHz
Quadrature Phase Error	F_{RF} = 1.9 GHz	−3	±1	+3	degree
I/Q Amplitude Imbalance	F_{RF} = 1.9 GHz		+0.3		dB
Noise Figure	Max Gain		11		dB
Mixer AGC Output Level	See Figure 34		24		mV p-p
Baseband DC Offset	At IMXO/QMXO, max gain (corrected, REF to VREF)		2		mV
Mixer Output Swing	Level at which IMD3 = 45 dBc				
	R_{LOAD} = 200 Ω		65		mV p-p
	R_{LOAD} = 1 kΩ		65		mV p-p
Mixer Output Impedance			3		Ω
BASEBAND OUTPUT AMPLIFIER	From IAIN to IOPP/IOPN and QAIN to QOPP/QOPN R_{LOAD} = 10 kΩ				
Gain			30		dB
Bandwidth	−3 dB (see Figure 22)		65		MHz
Output DC Offset (Differential)	(V_{IOPP} − V_{IOPN})	−200	±50	+200	mV
Common-Mode Offset	(V_{IOPP} + V_{IOPN})/2 − V_{VCMO}	−40	±5	+40	mV
Group Delay Flatness	0 MHz to 50 MHz		+1.8		ns p-p
Second-Order Intermod. Distortion	$F_{IN}1$ = 5 MHz, $F_{IN}2$ = 6 MHz, $V_{IN}1$ = $V_{IN}2$ = 8 mV p-p		−49		dBc
Third-Order Intermod. Distortion	$F_{IN}1$ = 5 MHz, $F_{IN}2$ = 6 MHz, $V_{IN}1$ = $V_{IN}2$ = 8 mV p-p		−67		dBc
Input Bias Current			+2		μA
Input Impedance			1‖3		MΩ‖pF
Output Swing Limit (Upper)		V_S − 1.3			V
Output Swing Limit (Lower)				0.4	V

Parameter	Conditions	Min	Typ	Max	Unit
CONTROL INPUT/OUTPUTS					
VCMO Input	@ V_S = 2.7 V		1		V
	@ V_S = 5 V	0.5	1	2.5	V
Gain Control Input Bias Current	VGIN		<1		µA
Offset Input Overriding Current	IOFS, QOFS		10		µA
VREF Output	R_{LOAD} = 10 kΩ	0.95	1.00	1.05	V
RESPONSE FROM RF INPUT TO FINAL BB AMP	IMXO and QMXO connected directly to IAIN and QAIN, respectively				
Gain @ V_{VGIN} = 0.2 V		65.5	69.5	72.5	dB
Gain @ V_{VGIN} = 1.2 V		−3	+0.5	+4	dB
Gain Slope		−96.5	−89	−82.5	dB/V
Gain Intercept	Linear extrapolation back to theoretical value at VGIN = 0	88	94	101	dB
LO/RF INPUT	(See Figure 30 through Figure 33 for more detail)				
LOIP Input Return Loss	Measuring LOIP LOIN, ac-coupled to ground with 100 pF.		−4		dB
	Measuring through evaluation board balun with termination		−9.5		dB
RFIP Input Return Loss	RFIP input pin		−10		dB
ENABLE					
Power-Up Control	Low = standby	0		0.5	V
Power-Up Control	High = enabled	+V_S − 1		+V_S	V
Power-Up Time	Time for final BB amps to be within 90% of final amplitude				
	@ V_S = 5 V		20		µs
	@ V_S = 2.7 V		10		µs
Power-Down Time	Time for supply current to be <4 mA				
	@ V_S = 5 V		30		µs
	@ V_S = 2.7 V		1.5		ms
POWER SUPPLIES	VPS1, VPS2, VPS3				
Voltage		2.7		5.5	V
Current (Enabled)	@ 5 V	48	64	80	mA
Current (Standby)	@ 5 V		400		µA
Current (Standby)	@ 3.3 V		80		µA

THEORY OF OPERATION

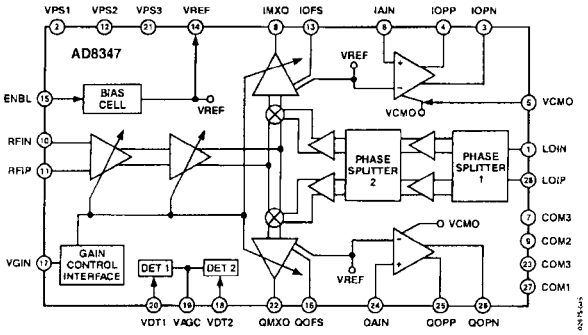

Figure 45. Block Diagram

The AD8347 is a direct I/Q demodulator usable in digital wireless communication systems including cellular, PCS, and digital video receivers. An RF signal in the frequency range of 800 MHz to 2,700 MHz is directly downconverted to the I and Q components at baseband using a local oscillator (LO) signal at the same frequency as the RF signal.

The RF input signal goes through two stages of variable gain amplifiers before splitting up to reach two Gilbert-cell mixers. The mixers are driven by a pair of LO signals which are in quadrature (90 degrees of phase difference). The outputs of the mixers are applied to baseband I-channel and Q-channel variable gain amplifiers. The outputs from these baseband variable gain amplifiers are brought out to pins for external filtering. The filter outputs are then applied to a pair of on-chip, fixed gain, baseband amplifiers. These amplifiers gain up the outputs from the external filters to a level compatible with most A-to-D converters. A sum of squares detector is available for use in an automatic gain control (AGC) loop to set the output level. The RF and baseband amplifiers provide approximately 69.5 dB of gain control range. Additional on-chip circuits allow the setting of the dc level at the I-channel and Q-channel baseband outputs, as well as nulling the dc offset at each channel.

RF VARIABLE GAIN AMPLIFIERS (VGA)

These amplifiers use the patented X-AMP® approach with NPN differential pairs separated by sections of resistive attenuators. The gain control is achieved through a gaussian interpolator where the control voltage sets the tail currents supplied to the various differential pairs according to the gain desired. In the first amplifier, the combined output currents from the transconductance cells go through a cascode stage to resistive loads with inductive peaking. In the second amplifier, the differential currents are split and fed to the two Gilbert-cell mixers through separate cascode stages.

MIXERS

Two double balanced Gilbert-cell mixers, one for each channel, perform the in-phase (I) and quadrature (Q) down conversion. Each mixer has four cross-connected transistor pairs that are terminated in resistive loads and feed the differential baseband variable gain amplifiers for each channel. The quadrature LO signals drive the bases of the mixer transistors.

BASEBAND VARIABLE GAIN AMPLIFIERS

The baseband VGAs also use the X-AMP approach with NPN differential pairs separated by sections of resistive attenuators. The same interpolator controlling the RF amplifiers controls the tail currents of the differential pairs. The outputs of these amplifiers are provided off chip for external filtering. Automatic offset nulling minimizes the dc offsets at both I- and Q-channels. The common-mode output voltage is set to the same level as the reference voltage (1.0 V) generated in the Bias cell, also made available at the VREF pin (see Figure 45).

OUTPUT AMPLIFIERS

The output amplifiers gain up the signal coming back from each of the external filters to a level compatible with most high speed A-to-D converters. These amplifiers are based on an active feedback design to achieve high gain bandwidth with low distortion.

LO AND PHASE SPLITTERS

The incoming LO signal is applied to a polyphase phase splitter to generate the LO signals for the I-channel and Q-channel mixers. The polyphase phase splitters are RC networks connected in a cyclical manner to achieve gain balance and phase quadrature. The wide operating frequency range of these phase splitters is achieved by cascading multiple sections of

these networks with staggered RC constants. Each branch goes through a buffer to make up for the loss and high frequency roll-off. The output from the buffers then goes into another polyphase phase splitter to enhance the accuracy of phase quadrature. Each LO signal is buffered again to drive the mixers.

OUTPUT LEVEL DETECTOR

To create an AGC voltage (VAGC), two signals proportional to the square of each output channel are summed together and compared to a built-in threshold. The inputs to this rms detector are referenced to VREF.

BIAS

An accurate reference circuit generates the reference currents used by the different sections. The reference circuit is controlled by an external power-up (ENBL) logic signal that, when set low, puts the whole chip into a sleep mode typically requiring less than 400 μA of supply current. The reference voltage (VREF) of 1.0 V, that serves as the common-mode reference for the baseband circuits, is made available for external use. The VREF pin should be decoupled with a 0.1 μF capacitor to ground.

Appendix B

Distance Measuring Equipment Theory

DME stands for Distance Measuring Equipment. The DME is a medium range civil navigation aid system. The DME system's main components are shown in block diagram form in Figure B.1. The DME system uses a time delay method for measuring the distance from an aircraft to a ground station. The aircraft begins determining its distance by transmitting short pulse pairs at a maximum of 150 pulse pairs per second on the receive frequency of the selected ground station. After a fixed 50 microseconds delay from the received pulse time, the ground station transmits a pulse pair back to the aircraft on a frequency either 63 MHz higher or lower than the aircraft's transmission frequency. By measuring the delay between the transmitted and received pulses, less 50 microseconds, the aircraft's DME unit can determine its distance from the ground station. This gives the slant-range distance rather than horizontal distance, but the latter can be computed from knowledge of the aircraft's altitude and the elevation of the ground station. The 50 microseconds delay called the *fundamental delay* is introduced so that an aircraft which is flying very close to the beacon can complete transmission of the encoded interrogating pulse pair, and then deactivates its own transmitter, before its receiver begins receiving the corresponding beacon reply pulses.

The DME system operates in the frequency range 962 to 1213 MHz. The *ground-to-air* transmissions are confined in the 962 - 1024 MHz and 1151 - 1213 MHz bands. The 1025 - 1150 MHz is for the *air-to-ground* portion of the service. **Sharing** this band are the radar transponder systems which use 1030 MHz for ground-to-air and 1090 MHz for air-to-ground. Secondary Surveillance Radars (SSR) or radar transponders are located in the ground and continuously transmit interrogation pulses. Any aircraft within range, that contains an operating transponder listens for a SSR signal and sends a 4 digit transponder code that identifies itself. The aircraft is then displayed as a tagged icon on the controller's radar screen.

Of interest to this project is the **air-to-ground** portion of the spectrum. This is because any transmitting aircraft responding to either a DME ground stations or a SSR transponder will interfere with any radio astronomy telescope in its line-of-sight.

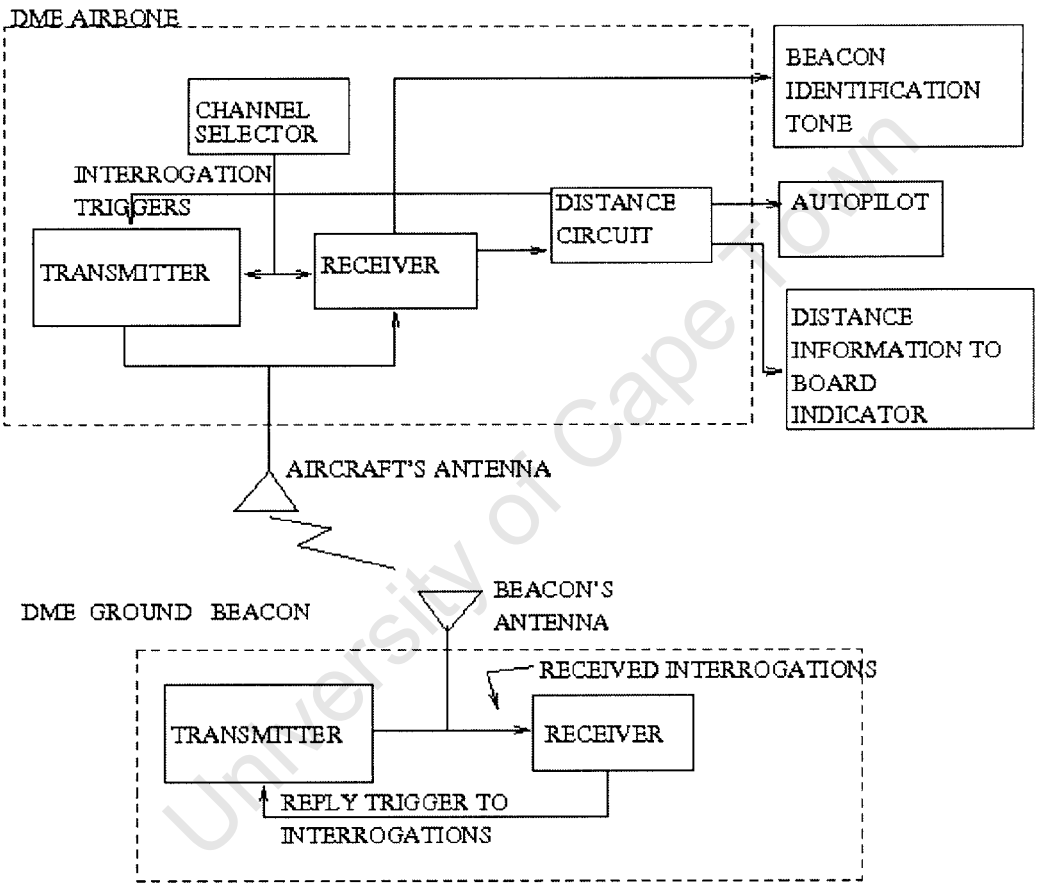

Figure B.1: DME System General Block Diagram.

B.1 DME Frequency Channels

DME transmission frequencies are 1 MHz apart. There are 126 *aircraft* transmission channels starting from channel 1 at 1025 MHz up to channel 126 at 1150 MHz. There are two transmission modes for each aircraft transmission channel, that is Mode X and Mode Y. In Mode X, the ground station transmission frequency is 63 MHz below the aircraft transmission frequency for channels 1-63 and 63 MHz above the aircraft frequency for channels 64-126. In Mode Y, the ground frequency is 63 MHz above the aircraft frequency for channels 1-63 and 63 MHz below the aircraft frequency for channels 64-126. Hence, in Mode Y the ground station transmissions are in the air-to-ground band. The illustration in Figure B.2 shows the DME Channels reply and interrogation frequencies. To render the system as immune as possible to errors caused by aircraft and ground station transmissions on the same frequency and random interferences, pulses are always transmitted in pairs.

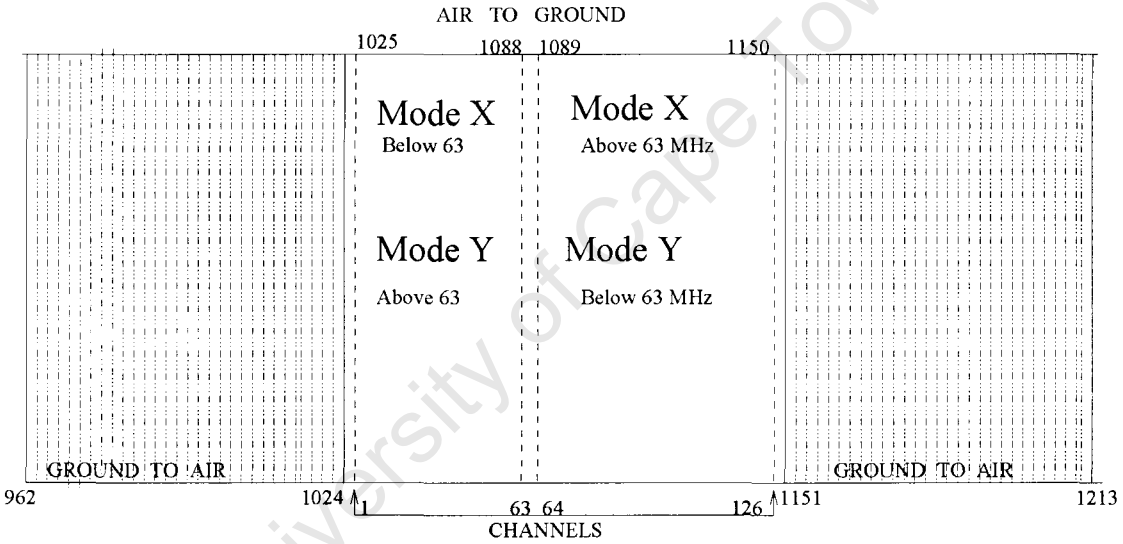

Figure B.2: DME Channels Reply and Interrogation Frequencies.

In Mode X:

- the interrogating (aircraft) pulses are 12 microseconds apart, and the reply (ground station) pulses are 12 microseconds apart.

In Mode Y:

- the interrogating (aircraft) pulses are 36 microseconds apart, and the reply (ground station) pulses are 30 microseconds apart.

B.2 DME Signal

B.2.1 Characteristics

According to the research done by Fisher [9] at the National Radio Astronomy Observatory using the Green Bank Telescope, the DME pulses are approximately Gaussian in shape as a function of time, with a half-amplitude full-width of 3.5 microseconds. The pulse is approximated by the following equation:

$$V(t)\ \alpha\ e^{-0.5(t/\sigma)^2} = e^{-2.7726(t/W)^2} \tag{B.1}$$

where t is time, and W is the full-width half-maximum pulse width in the same units as t.

B.2.2 Power

The DME peak pulse power is different for each aircraft depending on the manufacturer. However, the peak pulse power from a transmitter on a large jet aircraft is typically 300 watts [9]. The transmitter peak power for ground stations is between 100 Watts and 1000 Watts, depending on the station's intended service [9]. The voltage amplitude of the pulse in equation B.1 is one. Since peak pulse power for aircraft transmitters is 300 W, then assuming a 50 Ω impedance, the corresponding peak voltage is:

$$V_{\text{peak}} = \sqrt{P_{\text{peak}} R} = 122.5\,[\text{V}] \tag{B.2}$$

where R is the impedance. Therefore, the transmitted pulse from the aircraft is given by:

$$V(t) = 122.5 \times e^{-2.7726(t/W)^2}\,[\text{V}] \tag{B.3}$$

Appendix C

Simulation Tests Plots

The following plots show the power spectrum of the demodulated signal at different RF power levels for the same local oscillator frequency. The RF signal in all cases is the simulated DME signal and the receiver is at maximum gain.

C.1 DME Signal for Maximum Gain

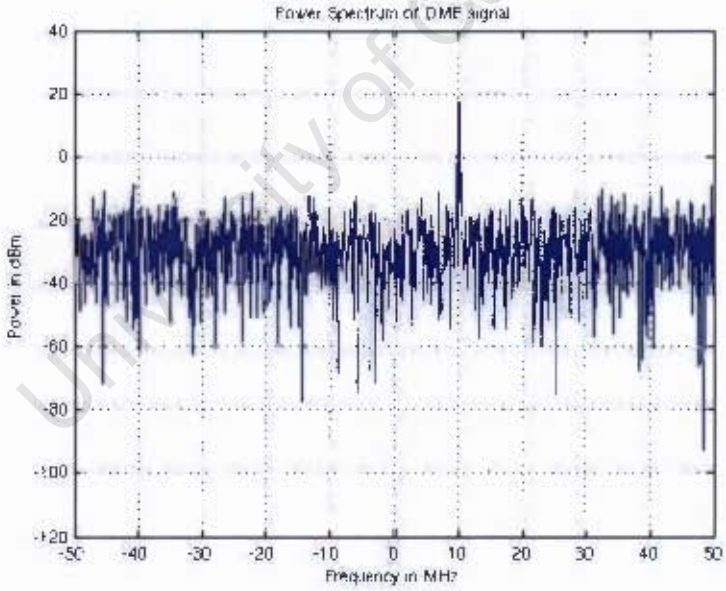

Figure C.1: Power spectrum of the IF output signal at 10 MHz for an input RF signal power at -90 dBm.

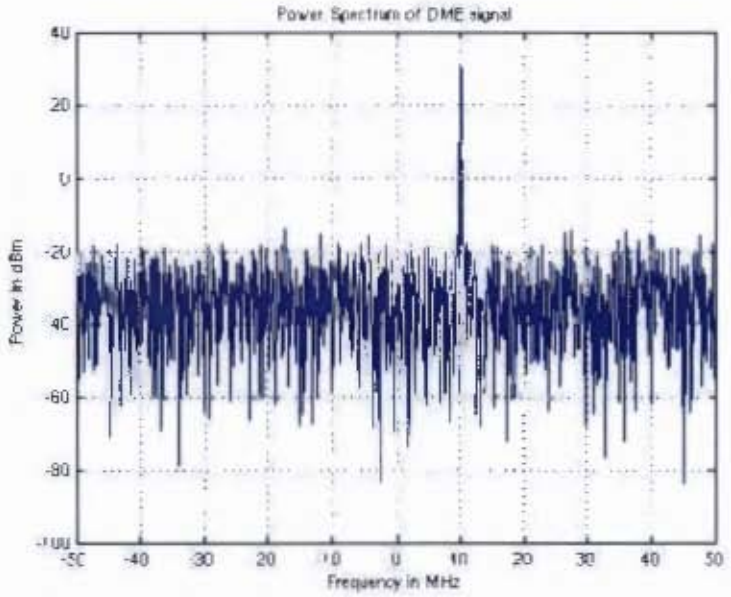

Figure C.2: Power spectrum of the IF output signal at 10 MHz for an input RF signal power at -80 dBm.

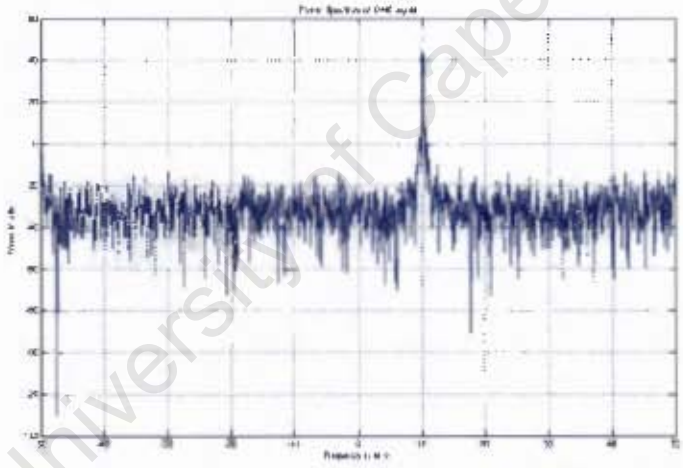

Figure C.3: Power spectrum of the IF output signal at 10 MHz for an input RF signal power at -70 dBm.

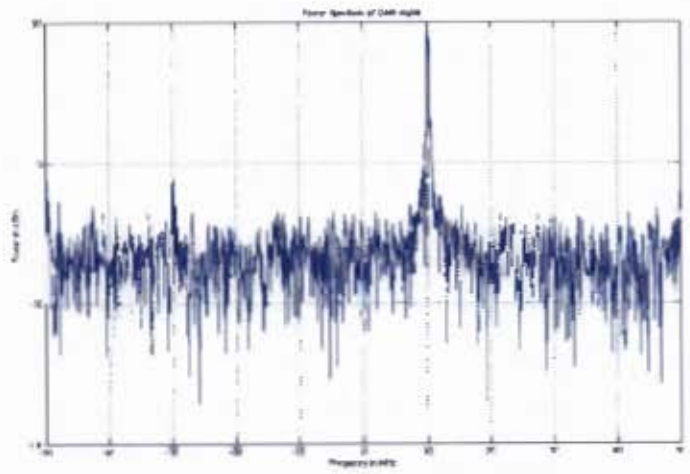

Figure C.4: Power spectrum of the IF output signal at 10 MHz for an input RF signal power at -60 dBm.

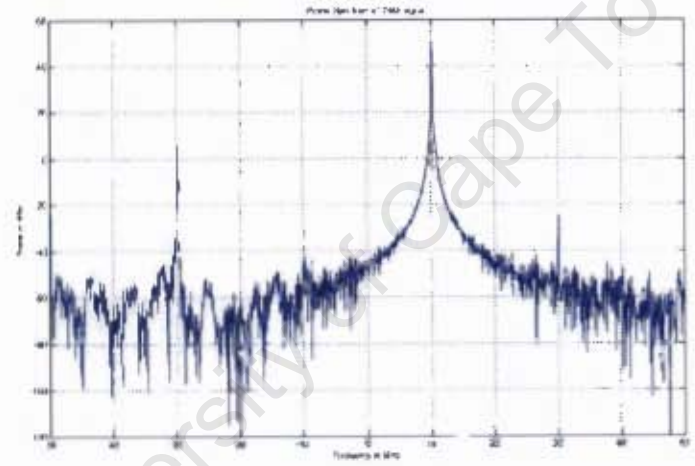

Figure C.5: Power spectrum of the IF output signal at 10 MHz for an input RF signal power at -58 dBm. The inter-modulation products are unacceptable above -58 dBm as described in Chapter 4.

C.2 Two-tone testing

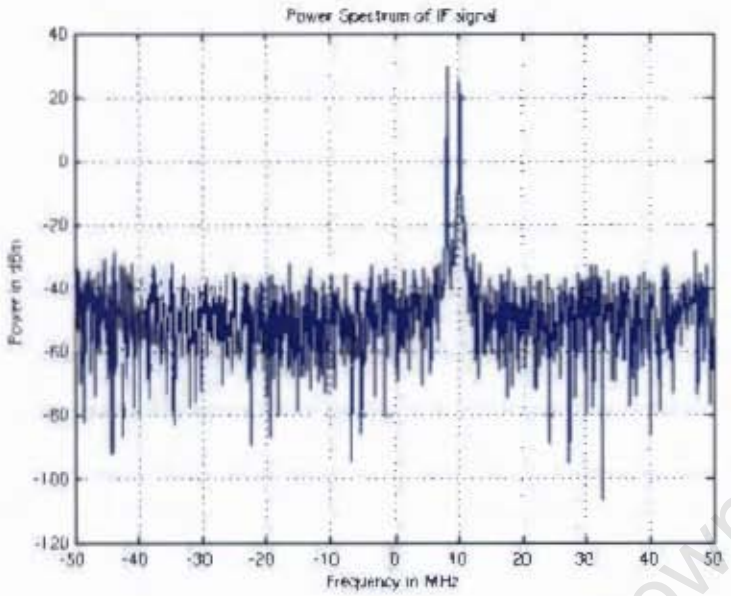

Figure C.6: Power spectrum of the IF output signals showing the locations and power levels of the 3rd-order products for an input RF signal power at -90 dBm.

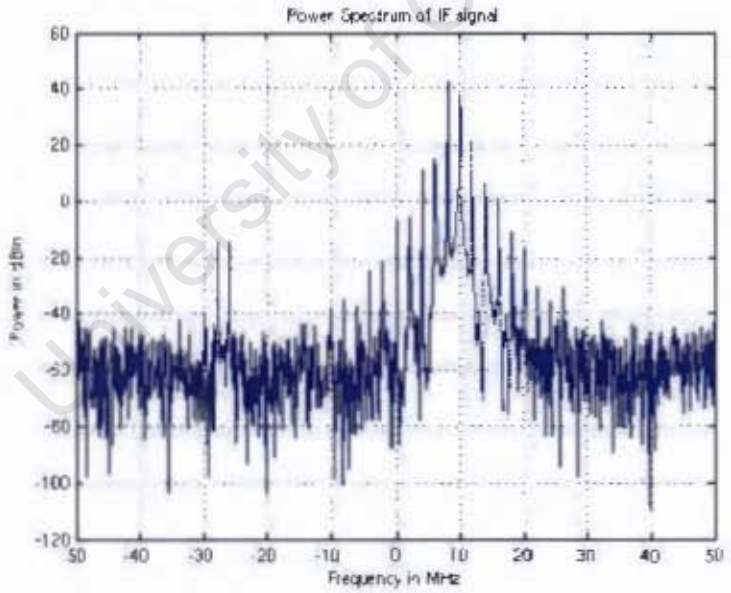

Figure C.7: Power spectrum of the IF output signals showing the locations and power levels of the 3rd-order products for an input RF signal power at -70 dBm.

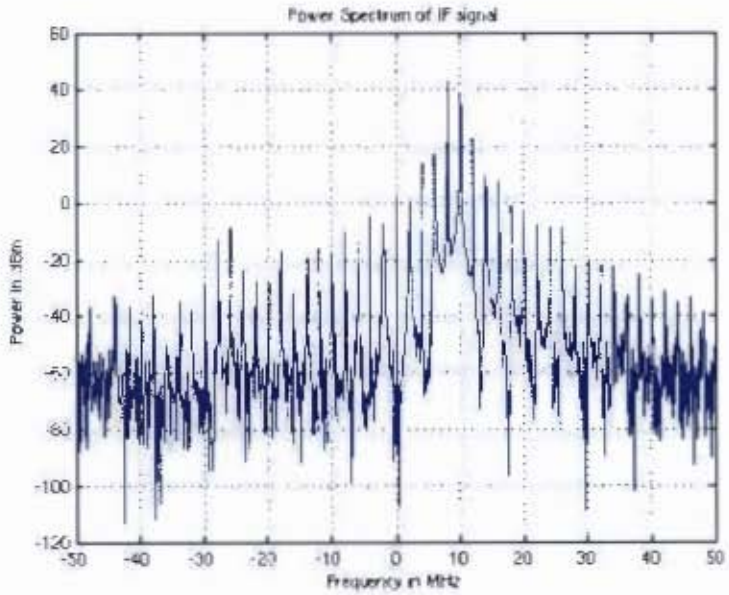

Figure C.8: Power spectrum of the IF output signals showing the locations and power levels of the 3rd-order products for an input RF signal power at -59 dBm. The 3rd-order products are very unacceptable.

Appendix D

Practical Tests Apparatus and Plots

D.1 Signal Generators Used

The following photographs show the signal generators that were used for the tests and how the equipment was set-up.

Figure D.1: The two signal generators used to produce the RF and LO signals. The bottom generator produces the LO signal.

Figure D.2: The receiver enclosure with the RF and LO connectors in the front. The In-phase and Quadrature signals from the demodulator are labelled Iout and Qout.

Figure D.3: The back of the PC where the digitiser is located. The I and Q signals are fed into the PCM 480 card that samples the two channels at 105 MSPS.

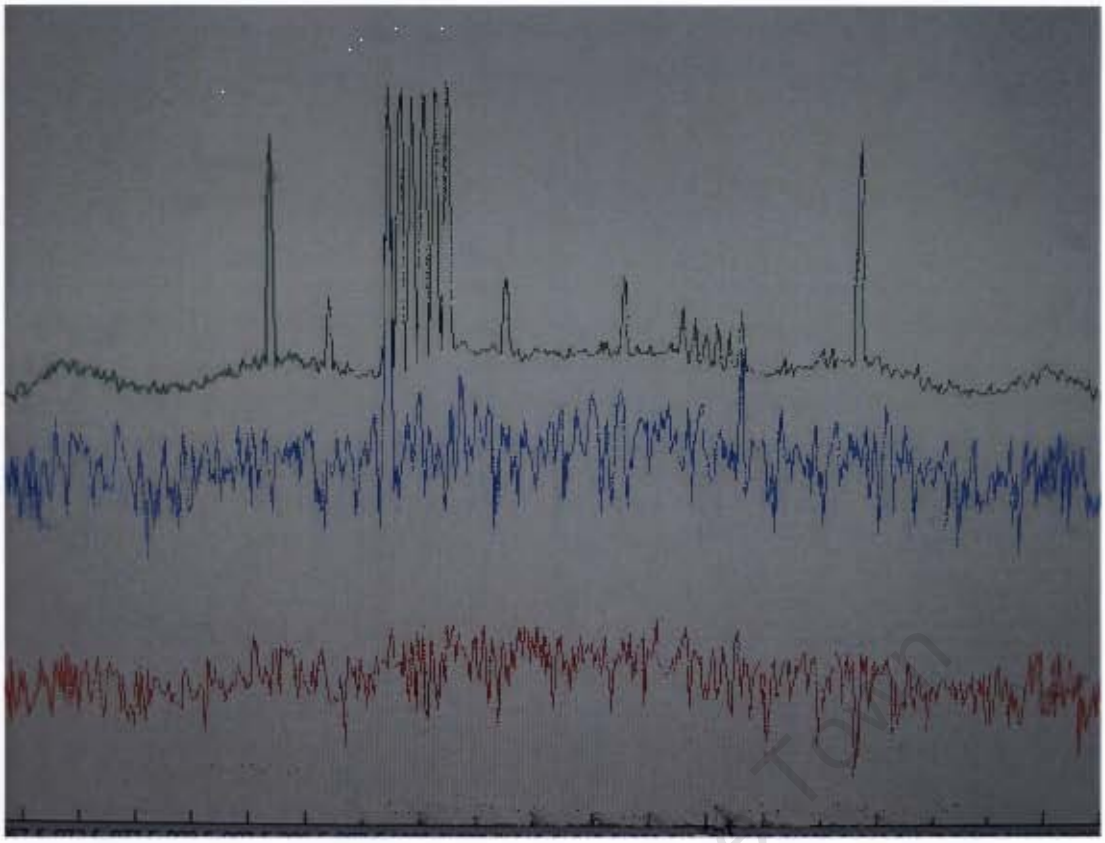

Figure D.4: The power spectrum plots of the demodulated signal from the purpose written software.

The red plot traces the minimum transients, the blue is the actual power level of the signal and the green plot traces the maximum signal. If the frequency of the RF or LO is varied the location of the IF changes as shown by the green plot.

D.2 Continuous Wave

The following plots serve to show the power spectrum of the IF signal for various RF signal power levels. The plots further serve to show the RF signal power levels that saturate the receiver under different modes and different receiver gain values.

D.2.1 Manual Mode

Minimum Gain

The LO frequency, 1020 MHz, represents 0 MHz in this figure (or is used as a reference taken to be equal to zero)

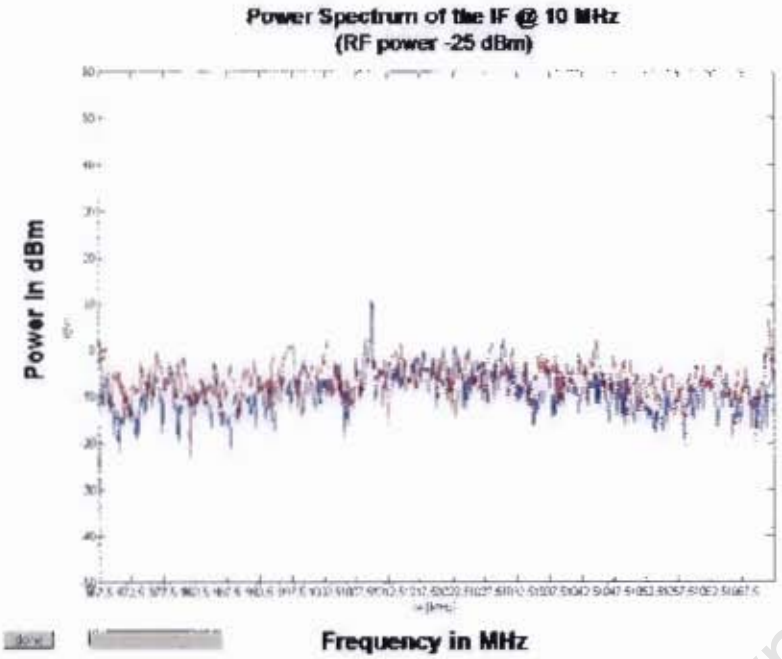

Figure D.5: Power spectrum of the output IF signal at 10 MHz (or 1010 MHz in the figure) for an RF input signal power of -25 dBm.

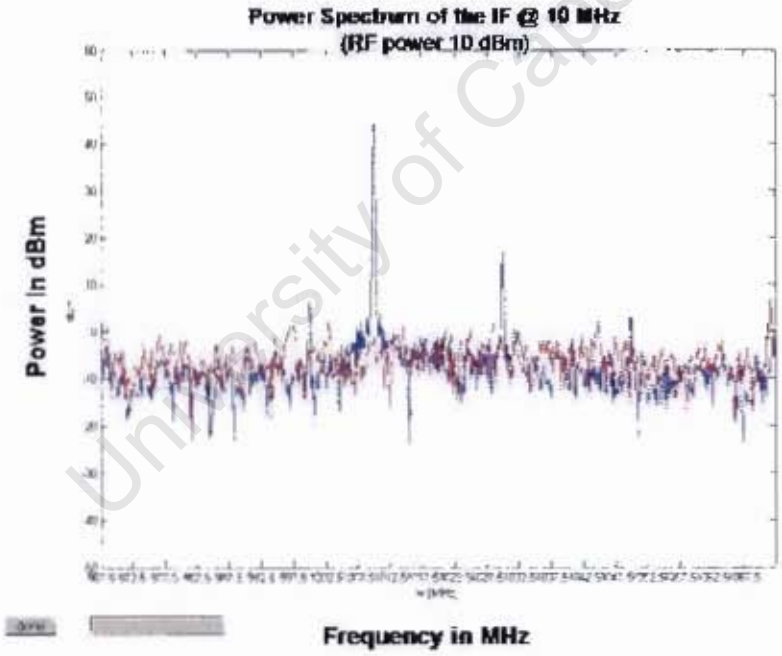

Figure D.6: Power spectrum of the output IF signal at 10 MHz (or 1010 MHz in the figure) for an RF input signal power of 10 dBm.

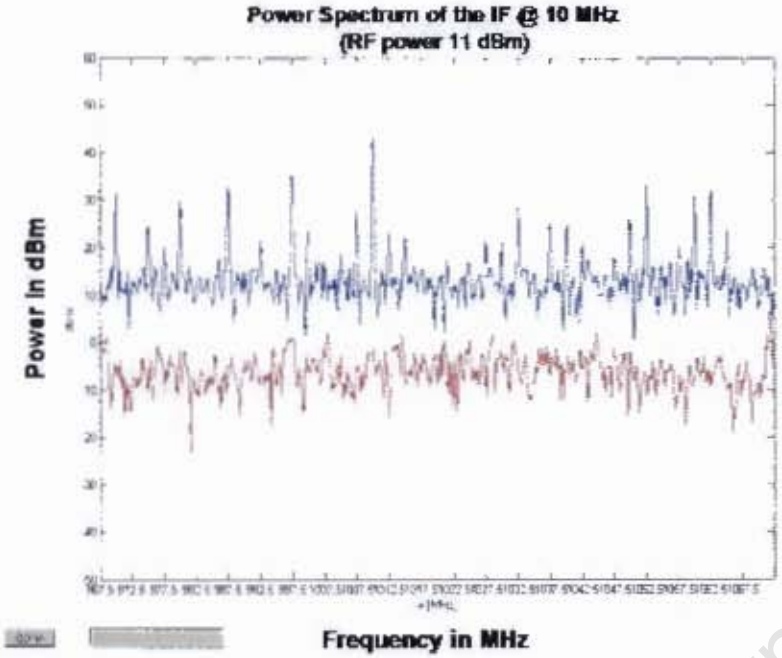

Figure D.7: Power spectrum of the output IF signal at 10 MHz (or 1010 MHz in the figure) for an RF input signal power of 12 dBm.

Maximum Gain

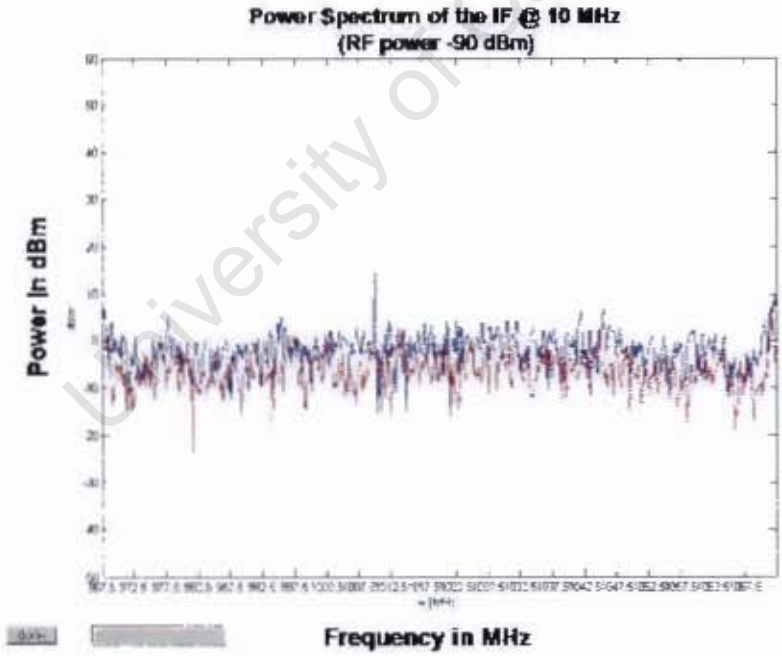

Figure D.8: Power spectrum of the output IF signal at 10 MHz (or 1010 MHz in the figure) for an RF input signal power of -90 dBm.

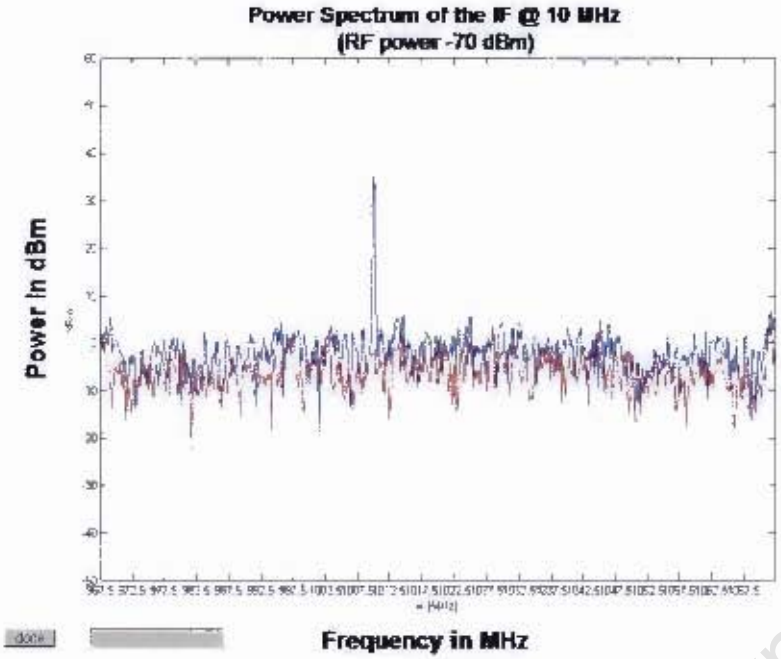

Figure D.9: Power spectrum of the output IF signal at 10 MHz (or 1010 MHz in the figure) for an RF input signal power of -70 dBm.

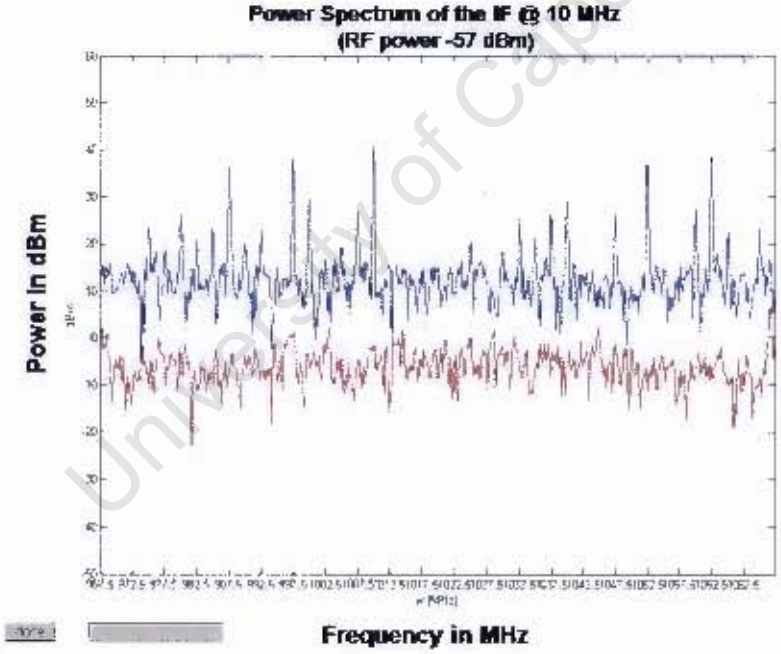

Figure D.10: Power spectrum of the output IF signal at 10 MHz (or 1010 MHz in the figure) for an RF input signal power of -57 dBm.

D.2.2 AGC Mode

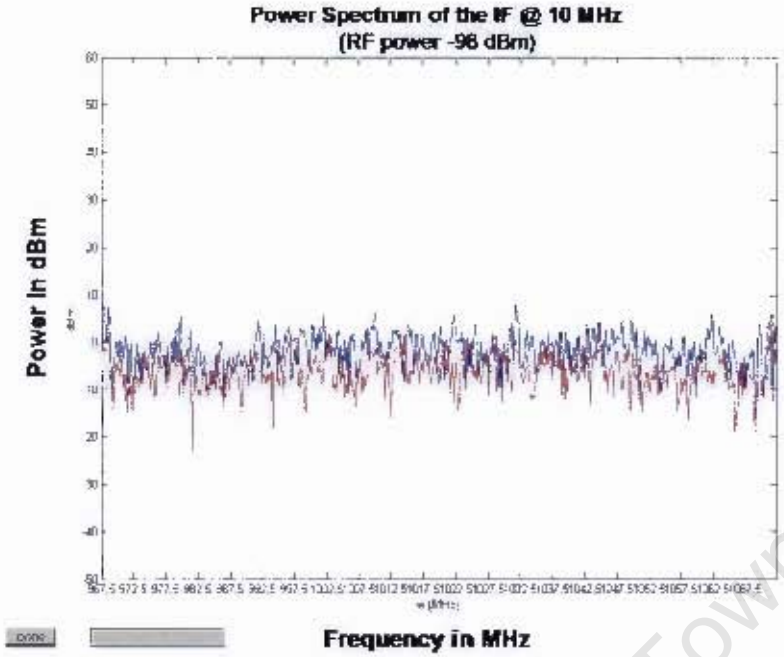

Figure D.11: Power spectrum of the output IF signal at 10 MHz (or 1010 MHz in the figure) for a RF input signal power of -98 dBm.

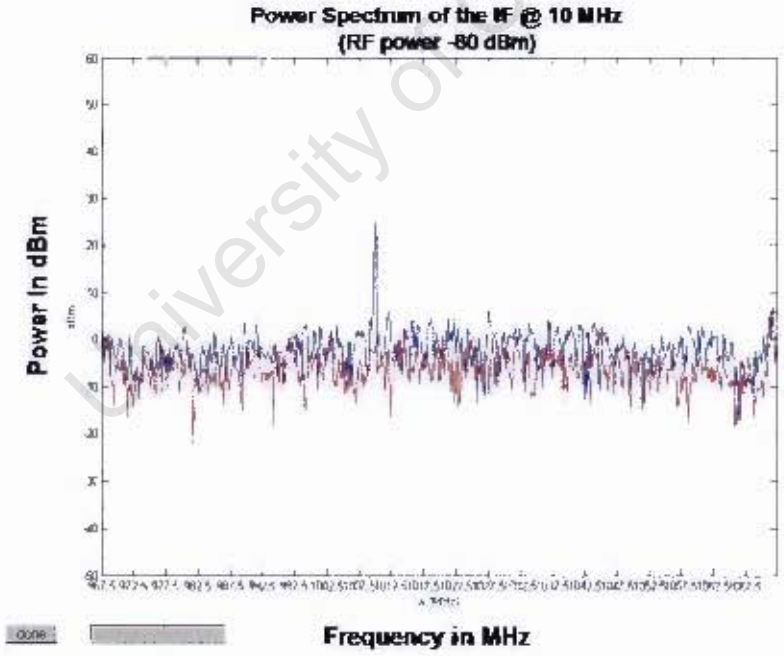

Figure D.12: Power spectrum of the output IF signal at 10 MHz (or 1010 MHz in the figure) for a RF input signal power of -80 dBm.

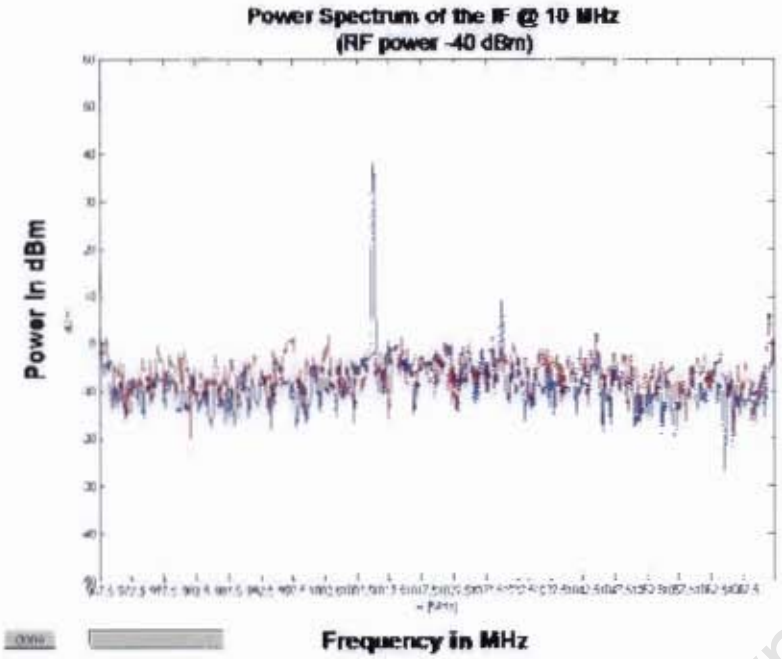

Figure D.13: Power spectrum of the output IF signal at 10 MHz (or 1010 MHz in the figure) for a RF input signal power of -40 dBm.

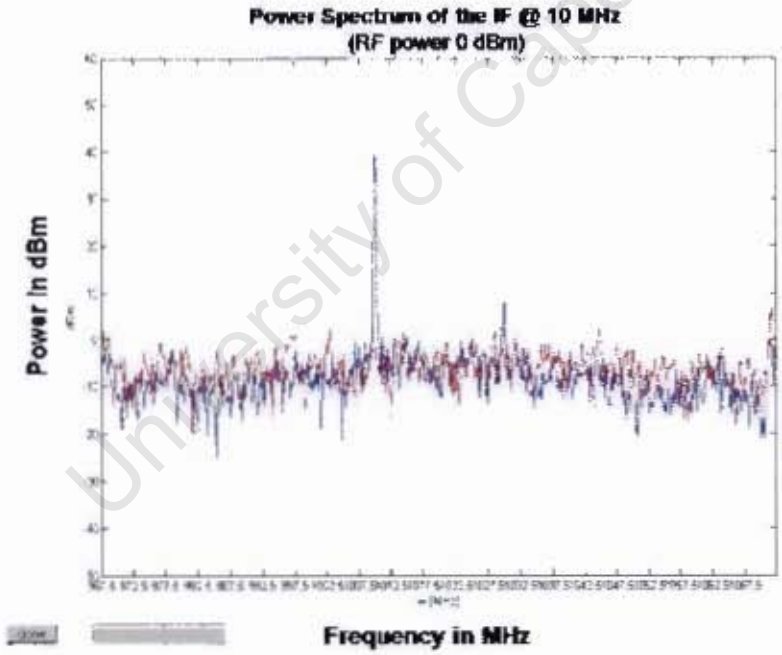

Figure D.14: Power spectrum of the output IF signal at 10 MHz (or 1010 MHz in the figure) for a RF input signal power of -40 dBm.

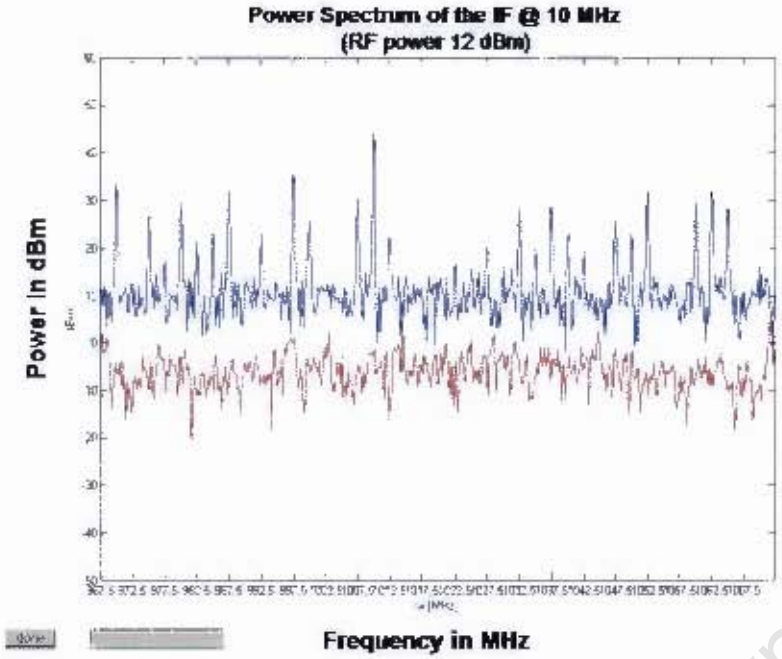

Figure D.15: Power spectrum of the output IF signal at 10 MHz (or 1010 MHz in the figure) for a RF input signal power of 12 dBm.

D.3 Amplitude Modulated DME like signals

D.3.1 AGC Mode

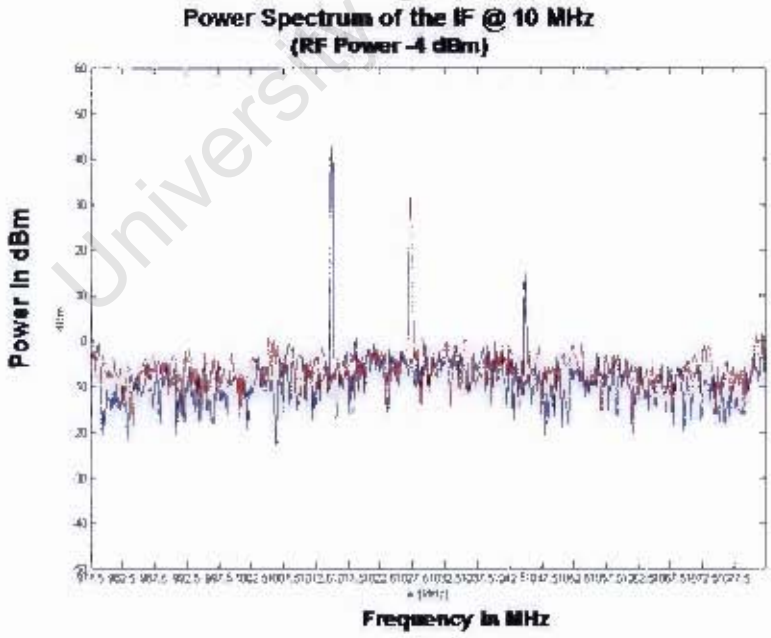

Figure D.16: Power spectrum of the output IF signal at 10 MHz (or 1000 MHz in the figure) for a RF input signal power of -4 dBm.

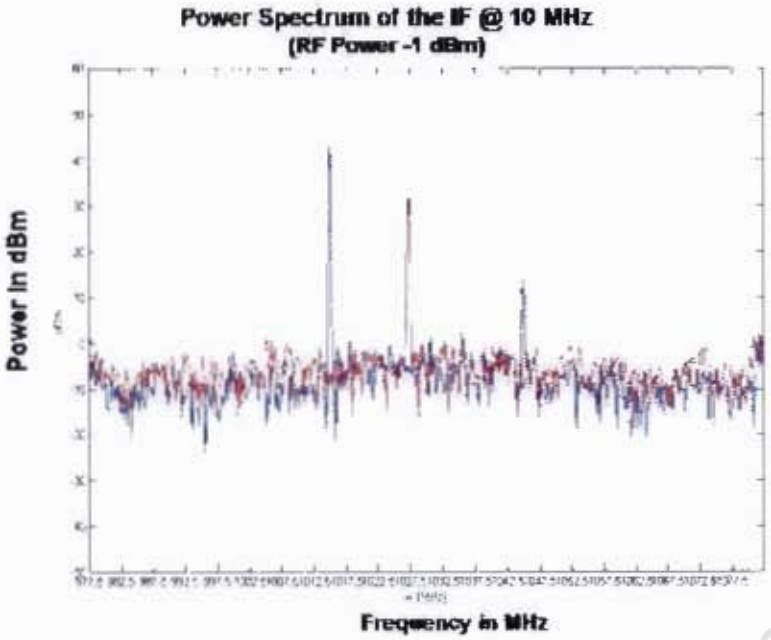

Figure D.17: Power spectrum of the output IF signal at 10 MHz (or 1000 MHz in the figure) for a RF input signal power of -1 dBm.

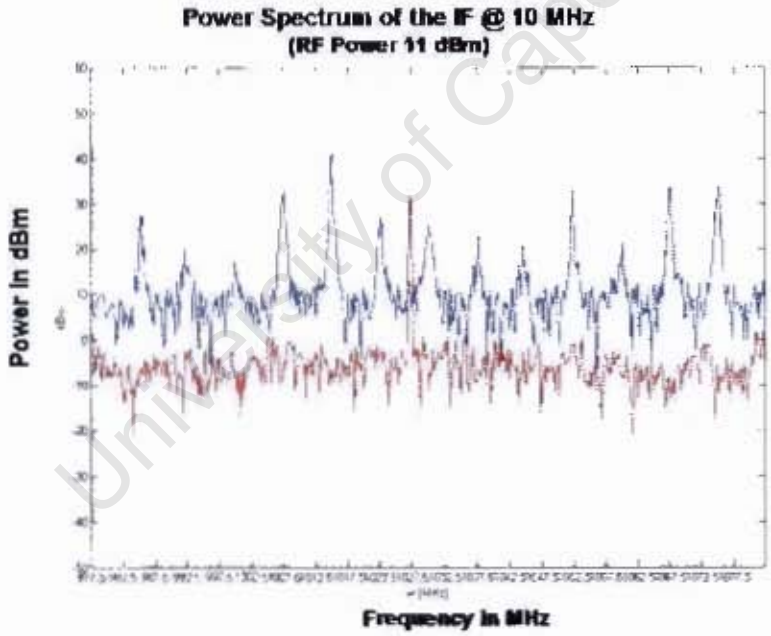

Figure D.18: Power spectrum of the output IF signal at 10 MHz (or 1000 MHz in the figure) for a RF input signal power of 11 dBm.

Appendix E

Matlab Signal Processing

The Matlab code used to combine the In-phase and Quadrature data from the simulation and produce a plot of the power spectrum of the IF signal versus the frequency is given below.

```
I = in-phase; % this is the text file that contains the in-phase data
Q = quadrature; % this is the text file that contains the in-phase data
Com = complex(I,Q);
Y = FFT(Com,1024);
Pyy = Y *.conj(Y)/1024;
PyydBm = 10*log(Pyy)+30; % convert to dBm
f = 100*(-512:511)./1024; % set the frequency range
plot(f,PyydBm); grid on
title('Power Spectrum of DME signal')
xlabel('Frequency in MHz')
ylabel('Power in dBm')
```